EUROPEAN ORGANIZATION FOR NUCLEAR RESEARCH

The Forward Muon Detector of L3

The L3 F/B Muon Group

Abstract

Nuclear Instruments and Methods A

The L3 F/B Muon Group

A.Adam,[14] M.Aguilar-Benitez,[9] J.Alarcon,[9] J.Alberdi,[9] V.Alexandrov,[13] A.Aloisio,[10] M.G.Alviggi,[10] H.Anderhub,[16] M.Ariza,[9] T.Azemoon,[3] T.Aziz,[5] F.Bakker,[2] S.Banerjee,[5] K.Banicz,[14] J.Barcala,[9] U.Becker,[6] J.Berdugo,[9] P.Berges,[6] B.L.Betev,[16] A.Biland,[16] G.J.Bobbink,[2] R.Bock,[1] A.Böhm,[1] V.Borissov,[13] K.Bosseler,[1] Ph.Bouvier,[7] E.Brambilla,[10] J.D.Burger,[6] C.Burgos,[9] J.Buskens,[2] J.C.Carlier,[7] G.Carlino,[10] J.Casaus,[9] N.Cavallo,[10] I.Cerjak,[2] M.Cerrada,[9] Y.H.Chang,[17] H.S.Chen,[4] S.R.Chendvankar,[5] V.Chvatchkine,[9] M.Daniel,[9] R.de Asmundis,[10] G.Decreuse,[6] K.Deiters,[15] L.Djambazov,[16] P.Duraffourg,[7] F.C.Erné,[2] H.Esser,[1] S.Ezekiev,[13] G.Faber,[16] M.Fabre,[15] G.Fernandez,[9] K.Freudenreich,[16§] M.Fritschi,[16] P.Garcia-Abia,[9] A.Gonzalez,[9] A.Gurtu,[5] L.J.Gutay,[14] Ch.Haller,[6] W.D.Herold,[15] J.Herrmann,[16] A.Hervé,[7] H.Hofer,[16] H.Hofer,[6] M.Hofer,[16] T.Hofer,[16] J.Homma,[2] U.Horisberger,[16] I.Horvath,[16] P.Ingenito,[15] V.Innocente,[10] I.Ioudine,[9] M.Jaspers,[2] P.de Jong,[6] W.Kaestli,[16] H.Kaspar,[15] V.Kitov,[13] A.C.König,[11] V.Koutsenko,[6] S.Lanzano,[10] C.Lapoint,[6] A.Lebedev,[6] P.Lecomte,[16] L.Lista,[10] K.Lübelsmeyer,[1] W.Lustermann,[15] J.M.Ma,[4] M.Milesi,[6] A.Molinero,[9] A.Montero,[9] R.Moore,[3] S.Nahn,[6] J.Navarrete,[9] M.Okle,[16] I.Orlinov,[13] D.Ostojic,[16] D.Pandoulas,[1] P.Paolucci,[10] P.Parascandolo,[10] G.Passeggio,[10] S.Patricelli,[10] D.Peach,[7] D.Piccolo,[10] L.Pigni,[7] H.Postema,[6] C.Puras,[9] D.Ren,[16] P.Rewiersma,[2] A.Rietmeyer,[2] K.Riles,[3] J.Risco,[9] A.Robohm,[16] J.Rodin,[6] U.Roeser,[16] L.Romero,[9] W.van Rossum,[2] H.Rykaczewski,[16] M.E.Sarakinos,[14] M.Sassowsky,[1] V.Schegelsky,[12] N.Scholz,[16] K.Schultze,[1] H.Schuylenburg,[2] C.Sciacca,[10] P.G.Seiler,[15] T.Siedenburg,[1] R.Siedling,[1] B.Smith,[6] V.Soulimov,[10] K.Sudhakar,[5] O.Syben,[1] M.Tonutti,[1] A.Udovcic,[16] J.Ulbricht,[16] L.Veillet,[7] M.Vergain,[6] G.Viertel,[16] H.P.von Gunten,[16] An.A.Vorobyov,[12] V.Vrankovic,[15] A.de Waard,[2] S.Waldmeier-Wicki,[16] W.Wallraff,[1] H.C.Walter,[15] J.C.Wang,[6] Z.L.Wei,[4] R.Wetter,[16] I.Weverling,[2] C.Willmott,[9] F.Wittgenstein,[7] R.J.Wu,[4] K.S.Yang,[4] L.Zhou,[4] Y.Zhou,[3] H.L.Zuang,[4]

1 I. Physikalisches Institut, RWTH, D-52056 Aachen, FRG
III. Physikalisches Institut, RWTH, D-52056 Aachen, FRG
2 National Institute for High Energy Physics, NIKHEF, and University of Amsterdam, NL-1009 DB Amsterdam, The Netherlands
3 University of Michigan, Ann Arbor, MI 48109, USA
4 Institute of High Energy Physics, IHEP, 100039 Beijing, China
5 Tata Institute of Fundamental Research, Bombay 400 005, India
6 Massachusetts Institute of Technology, Cambridge, MA 02139, USA
7 European Laboratory for Particle Physics, CERN, CH-1211 Geneva 23, Switzerland
8 University of Geneva, CH-1211 Geneva 4, Switzerland
9 Centro de Investigaciones Energeticas, Medioambientales y Tecnologicas, CIEMAT, E-28040 Madrid, Spain
10 INFN-Sezione di Napoli and University of Naples, I-80125 Naples, Italy
11 University of Nijmegen and NIKHEF, NL-6525 ED Nijmegen, The Netherlands
12 Nuclear Physics Institute, St. Petersburg, Russia
13 Bulgarian Academy of Sciences, Central Laboratory of Mechatronics and Instrumentation, BU-1113 Sofia, Bulgaria
14 Purdue University, West Lafayette, IN 47907, USA
15 Paul Scherrer Institut, PSI, CH-5232 Villigen, Switzerland
16 Eidgenössische Technische Hochschule, ETH Zürich, CH-8093 Zürich, Switzerland
17 High Energy Physics Group, Taiwan, China
§ Corresponding author. e-mail freuden at afsmail.cern.ch

Contents

1 Introduction

1.1 Physics requirements

1.2 Overview of the detector

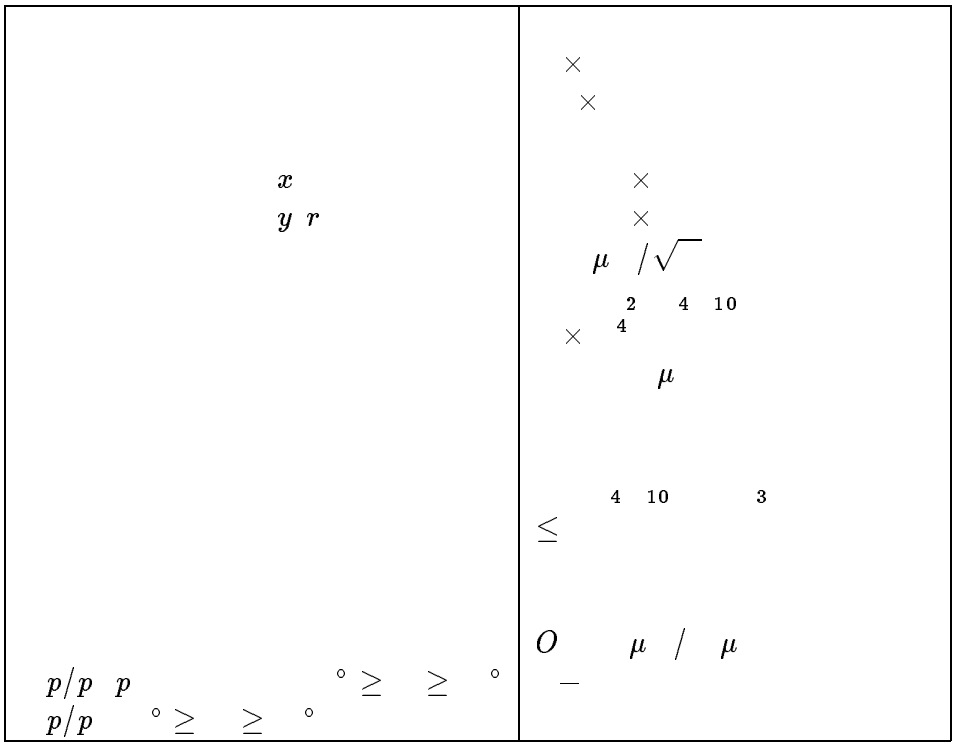

1.2.1 S-region : $^\circ \geq \geq ^\circ$

μ

μ

p

μ

1.2.2 T-region : $^\circ \geq \geq ^\circ$

1.3 Detector design considerations

μ μ

$\times$ ^{2}

$y-z$ [1)]

e^+e^-

$x-z$

μ $\sqrt{}$ μ

-
-
-
-

[1)] Octant by octant, we use a local coordinate system in which z coincides with the electron beam direction in LEP, y points radially outward along the octant centerline, and x is perpendicular to y and z. This corresponds approximately (along the octant centerline exactly) to $y = r$ and $x = \Phi$. The solenoidal magnetic field in L3 bends the muon in the $r-\Phi$ plane, the toroidal field bends in the $r-z$ plane.

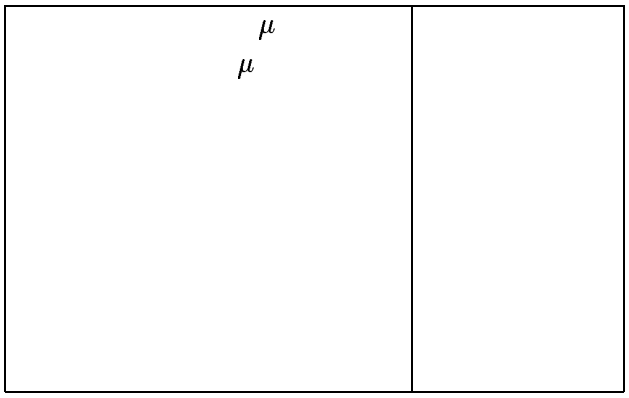

2 Drift Chambers

2.1 Design Principles

y

x

$t_1 \quad t_2$

$/v_{eff} \quad v_{eff}$

$x \qquad v_{eff} \times \quad t$

t

2 4 10

μ

μ

2.2 Calculation of Spatial Resolution

th

$\approx$

th

v . $/\mu$

μ

μ

3 Chamber construction and tests

3.1 Chamber enclosures

μ

3.2 Accurate wire positioning

μ

$\circ$

μ

μ

μ

3.3 Chamber wiring procedures

$\pm$

μ

3.4 Chamber tests

4 Infrastructure and Electronics

4.1 Front-end Boards and Amplifiers

M

$\times$ $/\mu$

$\times$. $\pm$.

. $\pm$.

$\times$

4.2 Discrimination Multiplexing and Readout

[2)]

[3)]

. μ

[2)] LECROY TDC LRS 1879
[3)] AD9696KR

4.3 Timing Calibration

≤ 1

≤ 1

4.4 High Voltage System

-
-
-
-

4)

μ

μ

4.5 Gas System

3

3/

3

4.6 Temperature monitor system

°

± . ° ° °

[4)] Connector type MSTB 2,5/4-STZ-5,08 produced by PHOENIX.

5 Trigger RPCs

5.1 The RPC System Layout

2

$\phi \simeq$

3

$\rho \simeq \quad . \quad ^{11}$

μ

5.2 Electronics and Tests

$\simeq$

5.3 Level-1 Trigger Generation and Data Readout

μ

$\simeq$

$\simeq$

[5]

$\times$

A_{ij}

$\cdot N_i \cdot N_j$ N_i N_j

[5] Each beam consisted of 4 trains with 2 to 4 bunchlets each. The bunchlets were separated by 247 ns.

6 F/B Toroids

6.1 Construction

×

2

6)

6.2 Magnetic field measurements

6) Metall Inert Gas welding

. .

6.3 Magnetic field calculation

°

$\leq R \leq$

$>$

7 System assembly and tests

7.1 Modules assembly

μ

7.2 Tests and Spatial Resolution

6

$|\theta_x| <$

$x \quad x_0 \pm v\ t - t_0 \qquad v \qquad . \qquad \mu$

t_0

σ μ

μ

σ

θ_x

$_{FM,FO}$ $-$ t_x t_w $\pm$. —— θ_x

t_x t_w

θ_x

$\frac{1}{2}$ FM FO

$\frac{1}{2}$ FO $-$ FM

σ . σ

t_0

t_0

7.3 Attachment to Doors

z

μ

7.4 Alignment systems

Relative alignment between FI, FM and FO layers: T-region

x

y

$\pm$. μ

x y

Alignment with respect to the central detector: S-region

z

x y

x y

μ μ z

μ z

- x

x μ

- y y

y

y μ

- z

μ

x y

7)

z

8) z

μ

μ

μ

μ x μ y μ z

8 Performance at LEP

$e^+e^- \to \mu^+\mu^- \gamma$

7) Type OPTIMESS 30LP by ELAG AG, Winterthur.

8) Type CR18-50K by DATAMEGA S.A., La Chaux de Fonds.

8.1 Muon track reconstruction

e^+e^- $^\circ <$ $^\circ -$ $<$

$^\circ$

t_0

t_0 t_0

T_0

T_0

T_0

e^+e^-

8.2 Characteristics of the data

$Z \rightarrow \mu^+\mu^-$

e^+e^- $\sqrt{s}$ E_b E_b

E_b

$x - y$

8.3 Spatial Resolution

e^+e^-

dy/dz dx/dz

χ^2/ndf

μ

σ_{core} $\pm$ μ $\pm$ μ

σ_{tail} $\pm$ μ $\pm$ μ

μ

μ x μ y dy/dz
dx/dz

8.4 Momentum Resolution

$E_{beam}/\ q \cdot p_{muon}$

E_{beam} p_{muon}

q

$^\circ <$ $<$ $^\circ$

$^\circ <$ $<$ $^\circ$

$E_{beam}/\ q \cdot p_{muon}$ $\pm$.
E/p

$\delta p/p$

$\delta p/p$

. .

8.5 RPC Performance

8.5.1 F/B trigger efficiency

$\pm$

ϵ_{dimuon} . $\pm$. ϵ_{single} . $\pm$.

8.5.2 Spatial resolution and detector efficiency

. $-$. kV

μ . $\pm$.

y

σ_y . $\pm$.

$\sigma_{y,1}$. $\pm$.

$\sigma_{y,2}$. $\pm$. $\sigma_{y,3}$. $\pm$.

ϵ . $\pm$.

8.5.3 Time resolution and bunchlet identification

-
-
-

$/v_p$.

σ . $\pm$.

9 Summary

10 Acknowledgement

References

A309

GARFIELD, a drift-chamber simulation program

A324

the GEANE program

List of Figures

σ σ $\times \sqrt{\mu}$ μ . . .

. . . . . .

. . . . . .

. . . . . .

x y z . . . . . .

μ

. . . . . .

. . . . . .

$x - y$

. . . . . .

. . . . . .

$e^+e^- \rightarrow \mu^+\mu^- \gamma$

$E_{beam}/\ q \cdot p_{muon}$ E_{beam}

q p_{muon}

. . . . . .

.

. . . . . .

. . . . . .

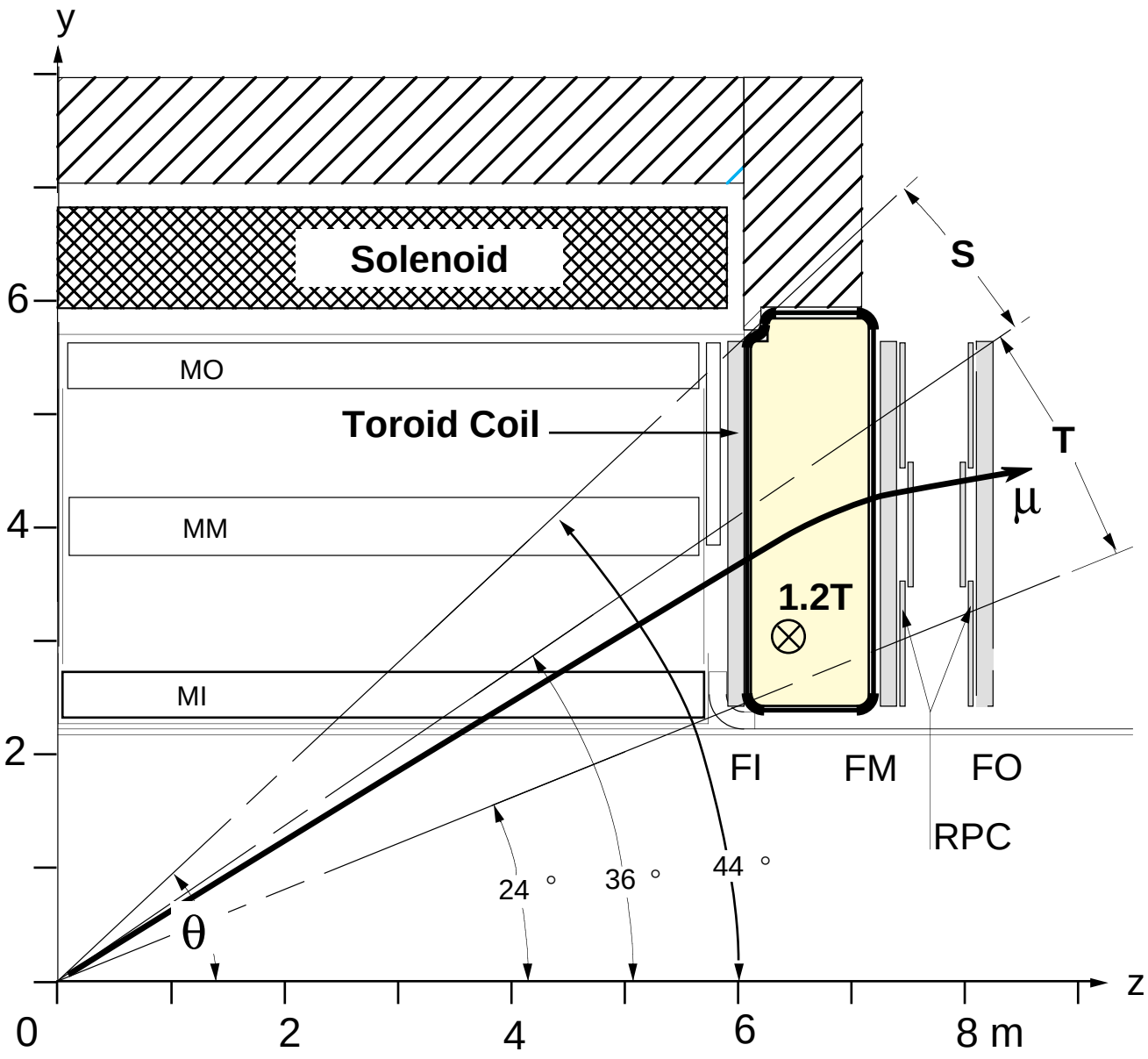
y
Solenoid
S
MO
Toroid Coil
T
μ
MM
1.2T
MI
FI
FM
FO
RPC
24 °
36 °
44 °
θ
z
0
2
4
6
8 m
2
4
6

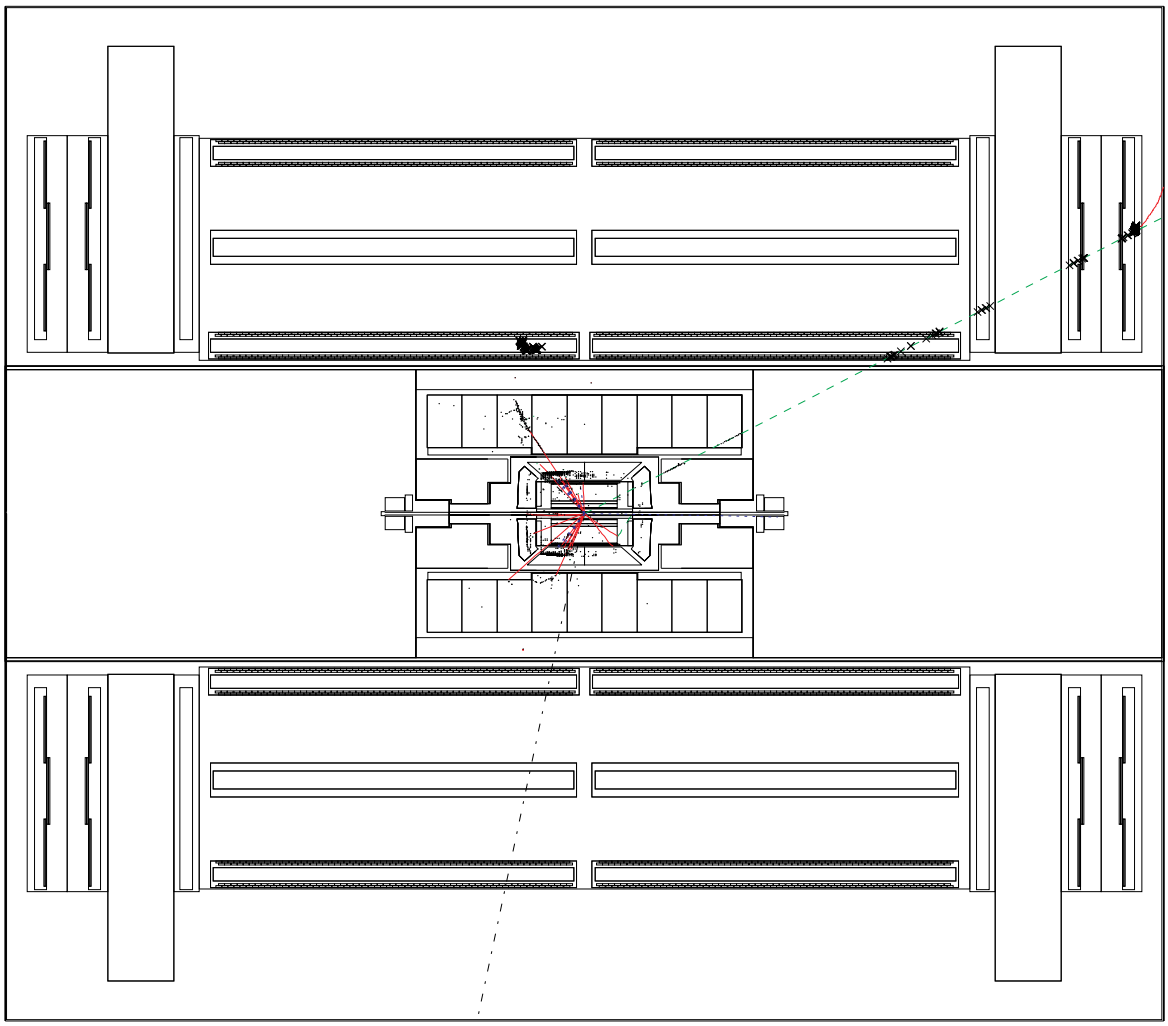

$+\ -\ \rightarrow\quad +\quad -\ \rightarrow \mu\nu_{\mu}$

ν_{μ}

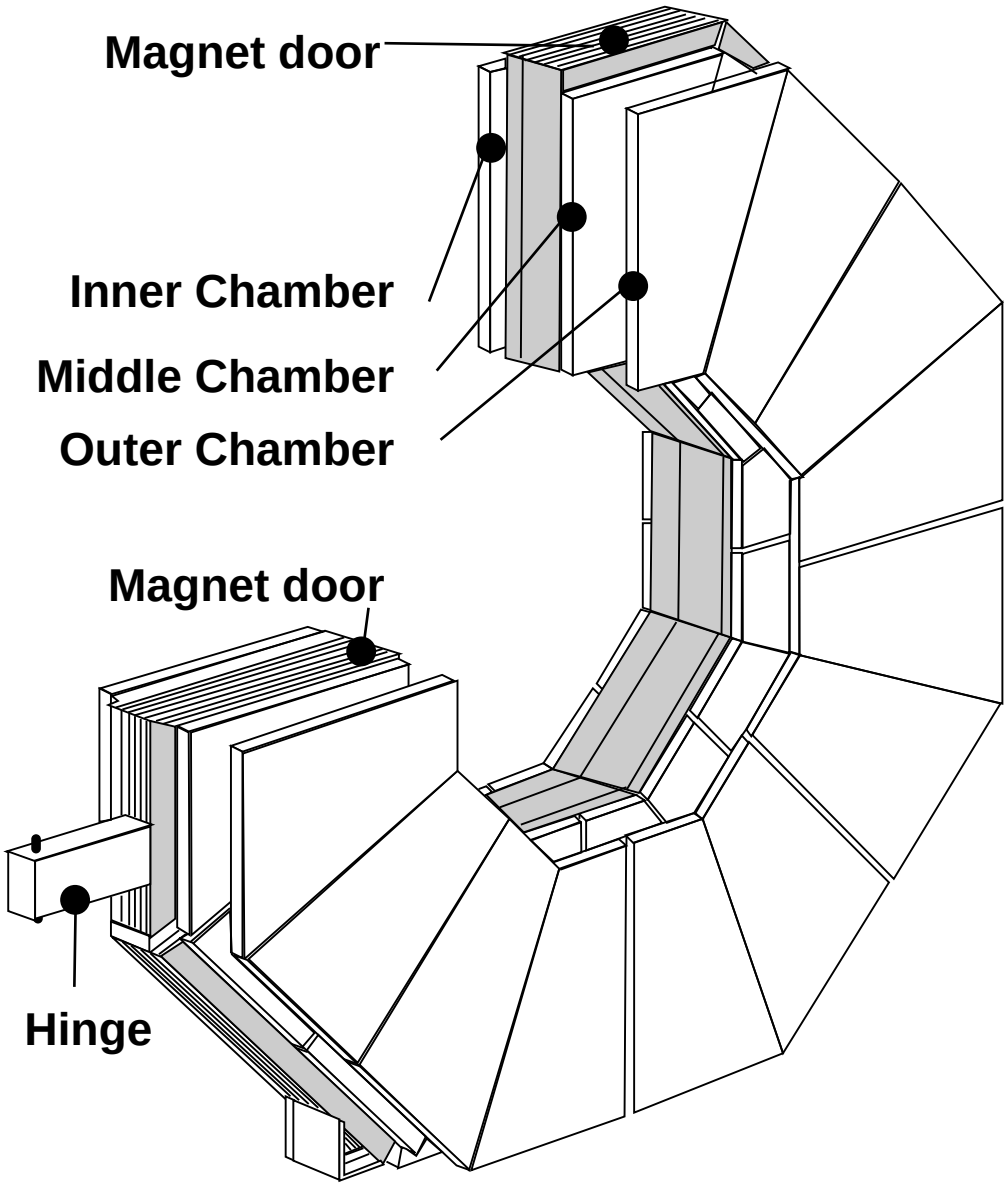
Magnet door
Inner Chamber
Middle Chamber
Outer Chamber
Magnet door
Hinge

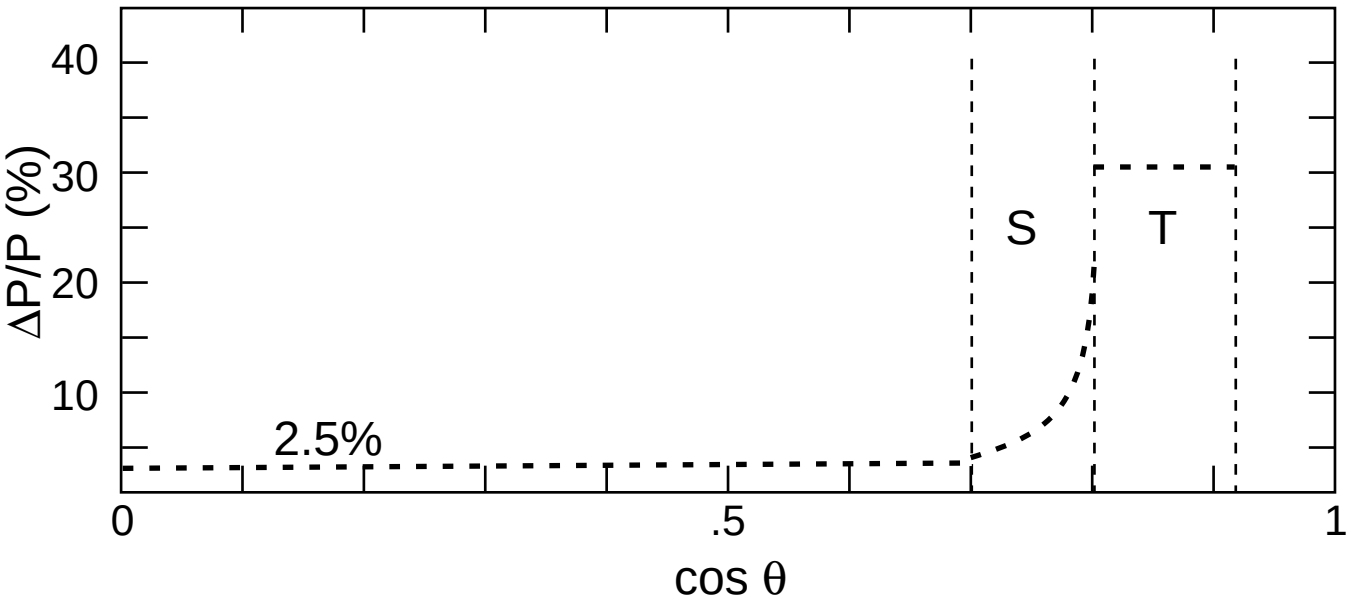
40
30
20
10
ΔP/P (%)
2.5%
S
T
0
.5
1
cos θ

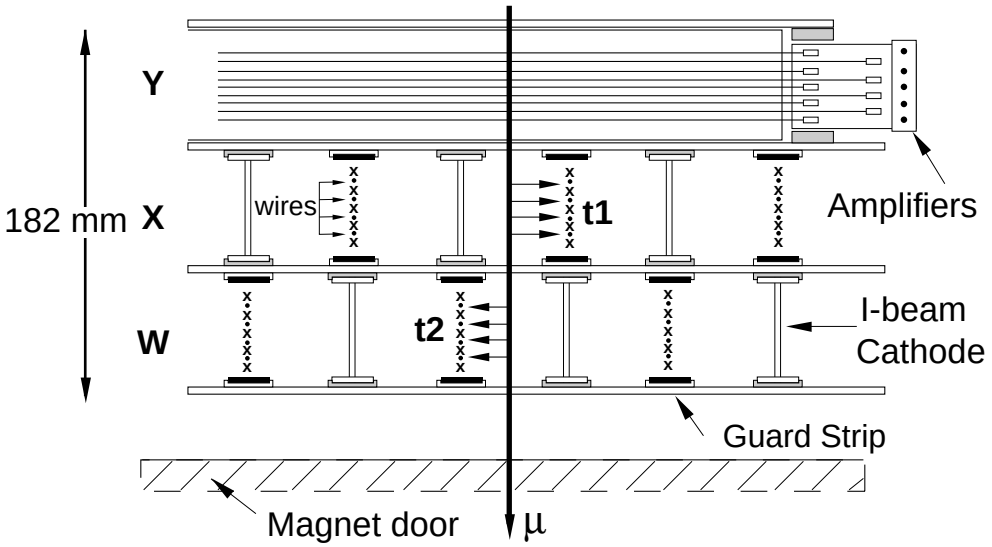
Y
182 mm
X
W
wires
t1
t2
Amplifiers
I-beam
Cathode
Guard Strip
Magnet door
μ

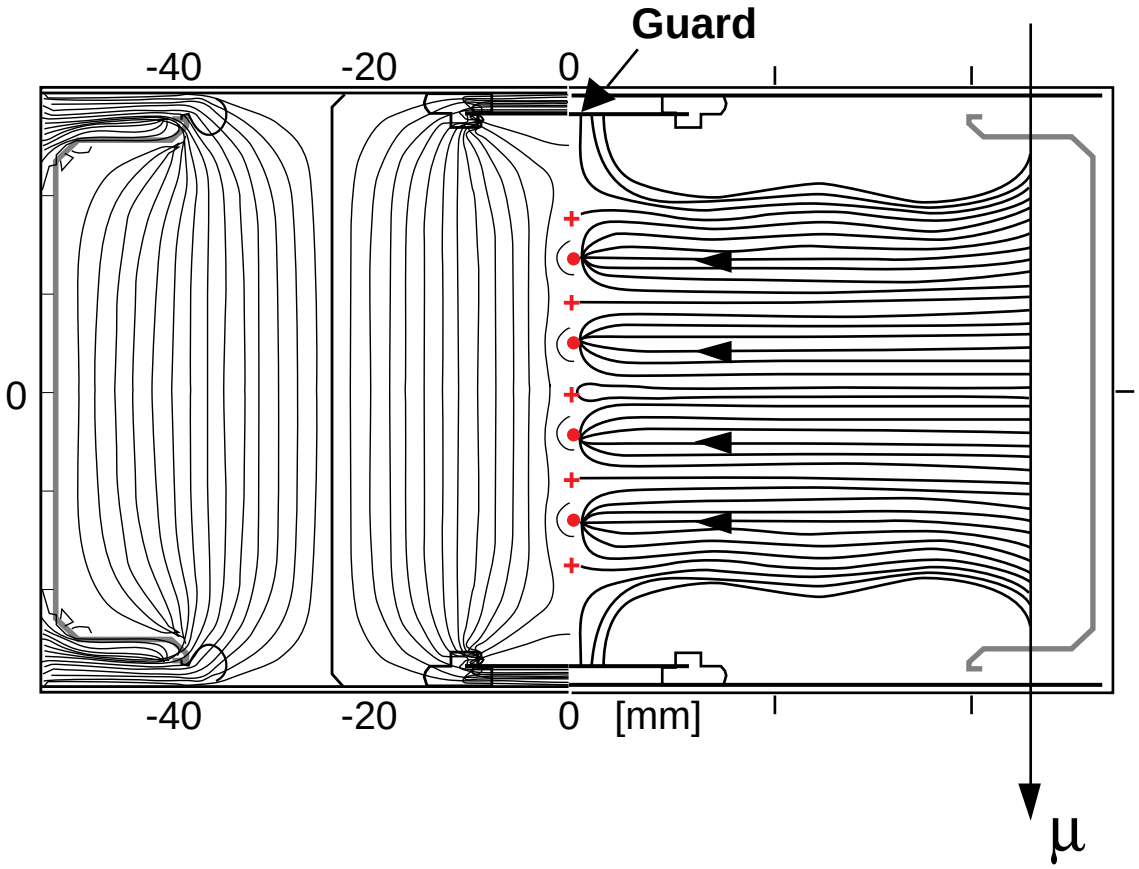
Guard
-40
-20
0
0
-40
-20
0
[mm]
μ

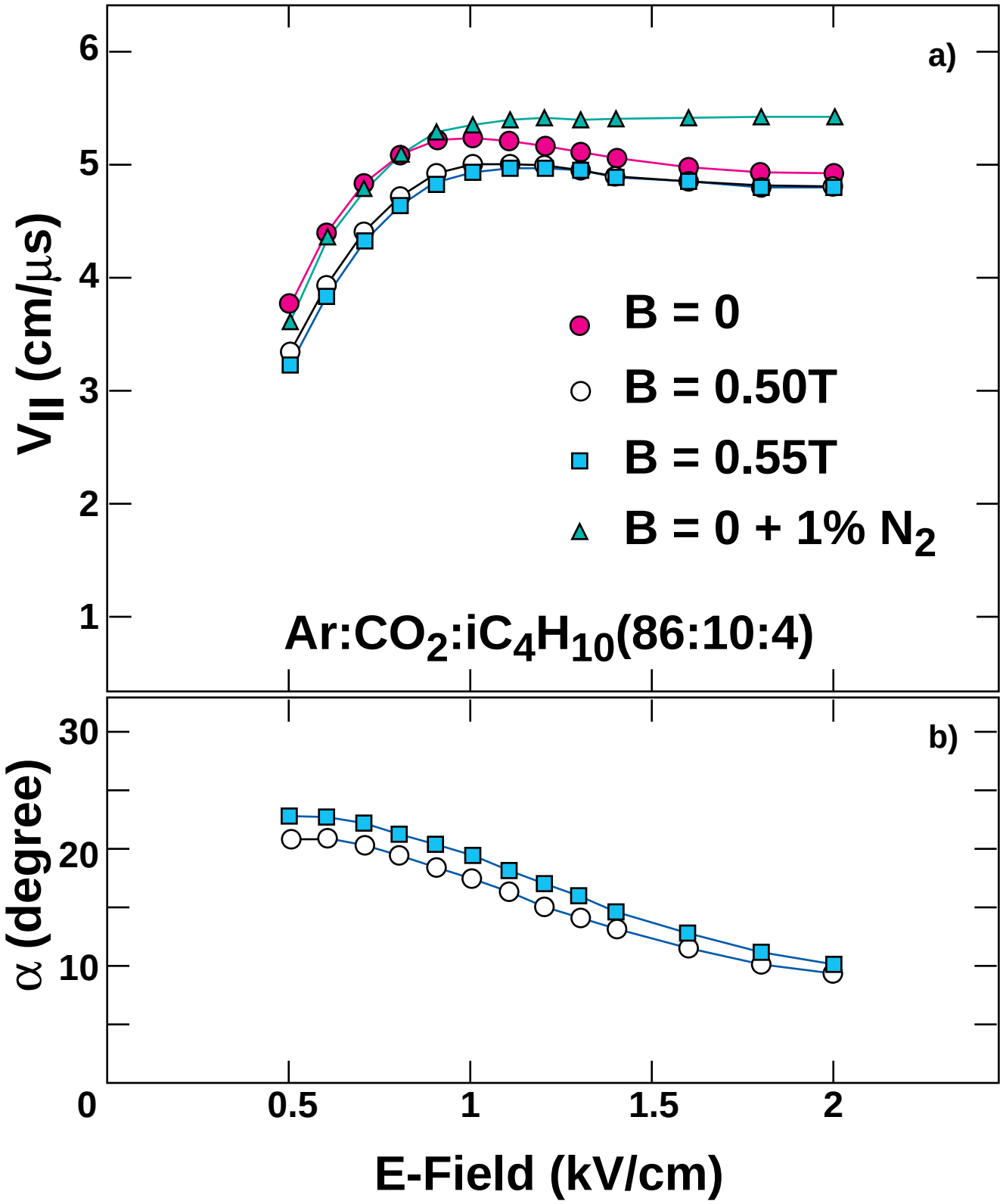
a)
b)
V_{II} (cm/μs)
α (degree)
E-Field (kV/cm)
B = 0
B = 0.50T
B = 0.55T
B = 0 + 1% N_2
Ar:CO_2:iC_4H_{10}(86:10:4)
6
5
4
3
2
1
30
20
10
0
0.5
1
1.5
2

N_2

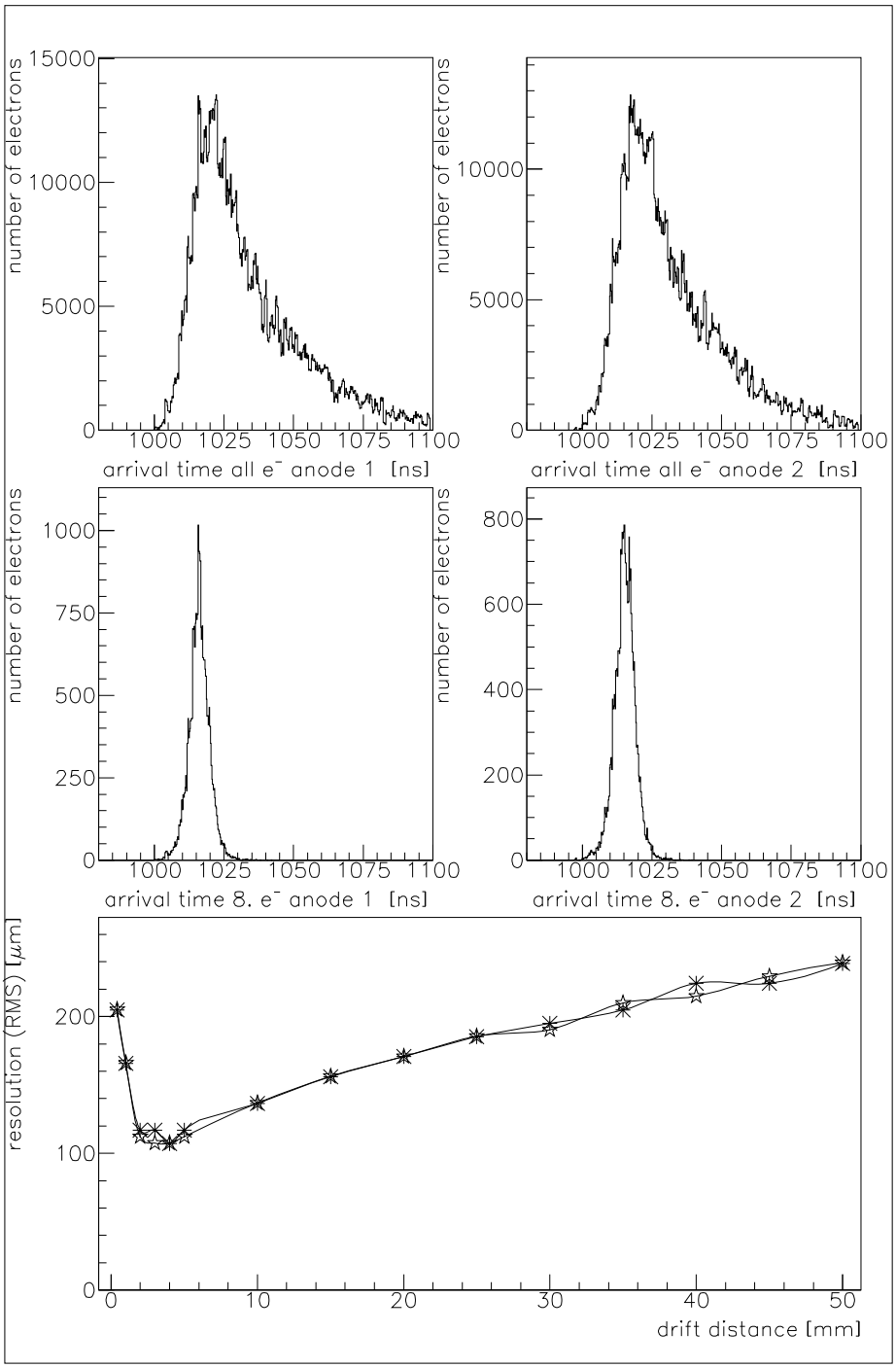
number of electrons
arrival time all e⁻ anode 1 [ns]
arrival time all e⁻ anode 2 [ns]
arrival time 8. e⁻ anode 1 [ns]
arrival time 8. e⁻ anode 2 [ns]
resolution (RMS) [μm]
drift distance [mm]

th

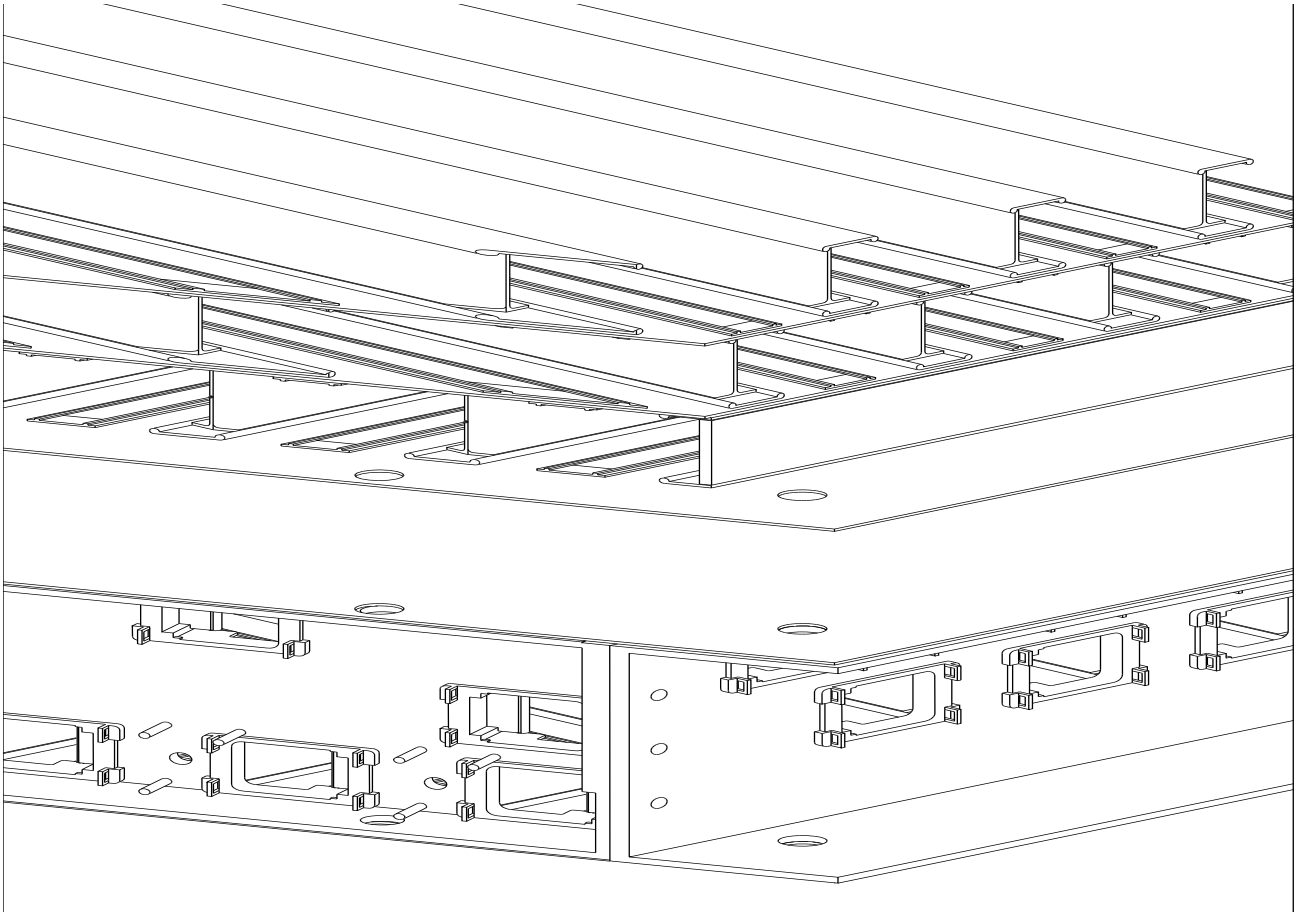

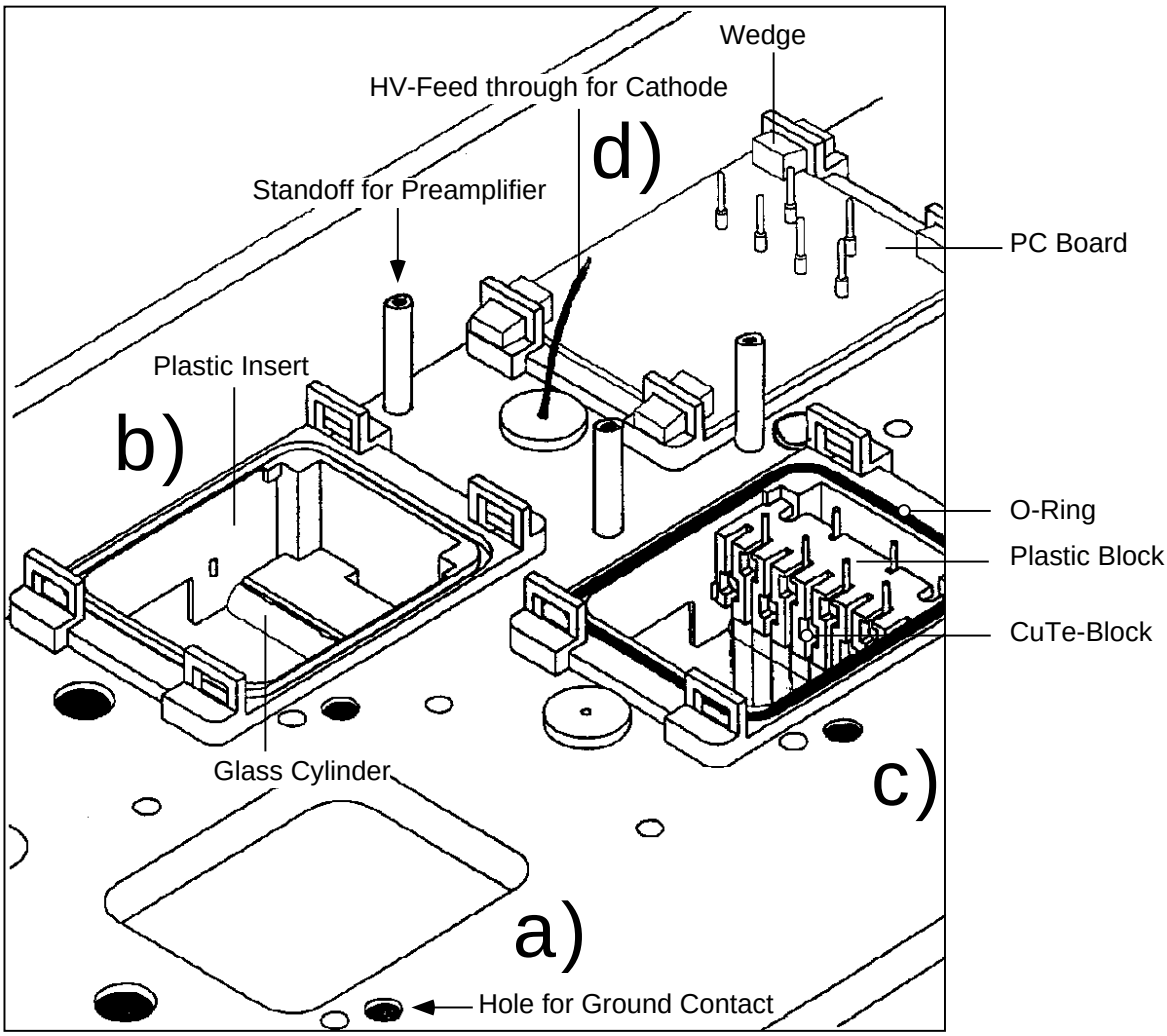
Wedge
HV-Feed through for Cathode
d)
Standoff for Preamplifier
PC Board
Plastic Insert
b)
O-Ring
Plastic Block
CuTe-Block
Glass Cylinder
c)
a)
Hole for Ground Contact

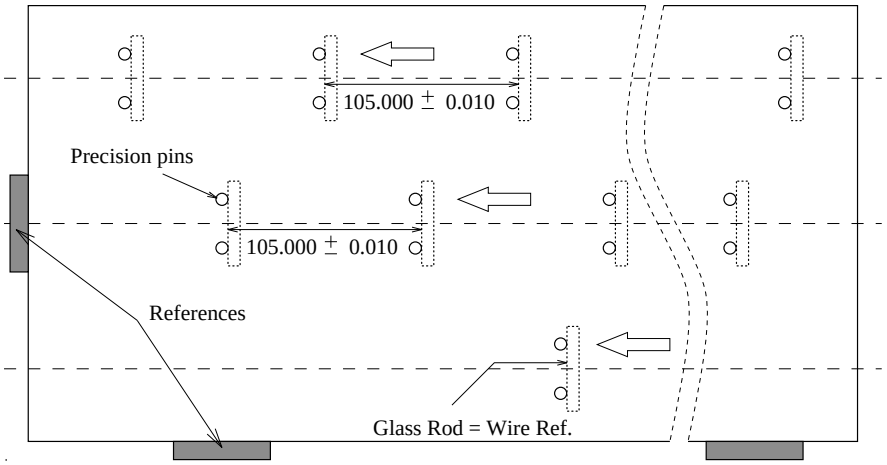
105.000 ± 0.010
Precision pins
105.000 ± 0.010
References
Glass Rod = Wire Ref.

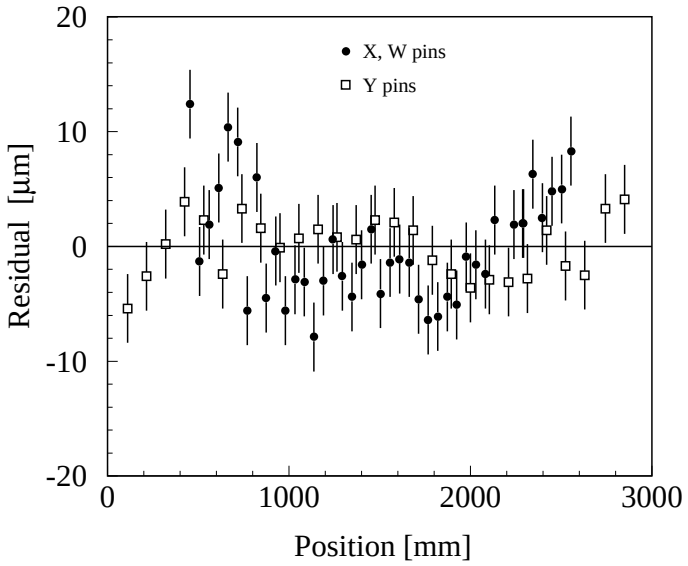
X, W pins
Y pins
Residual [μm]
Position [mm]
20
10
0
-10
-20
0
1000
2000
3000

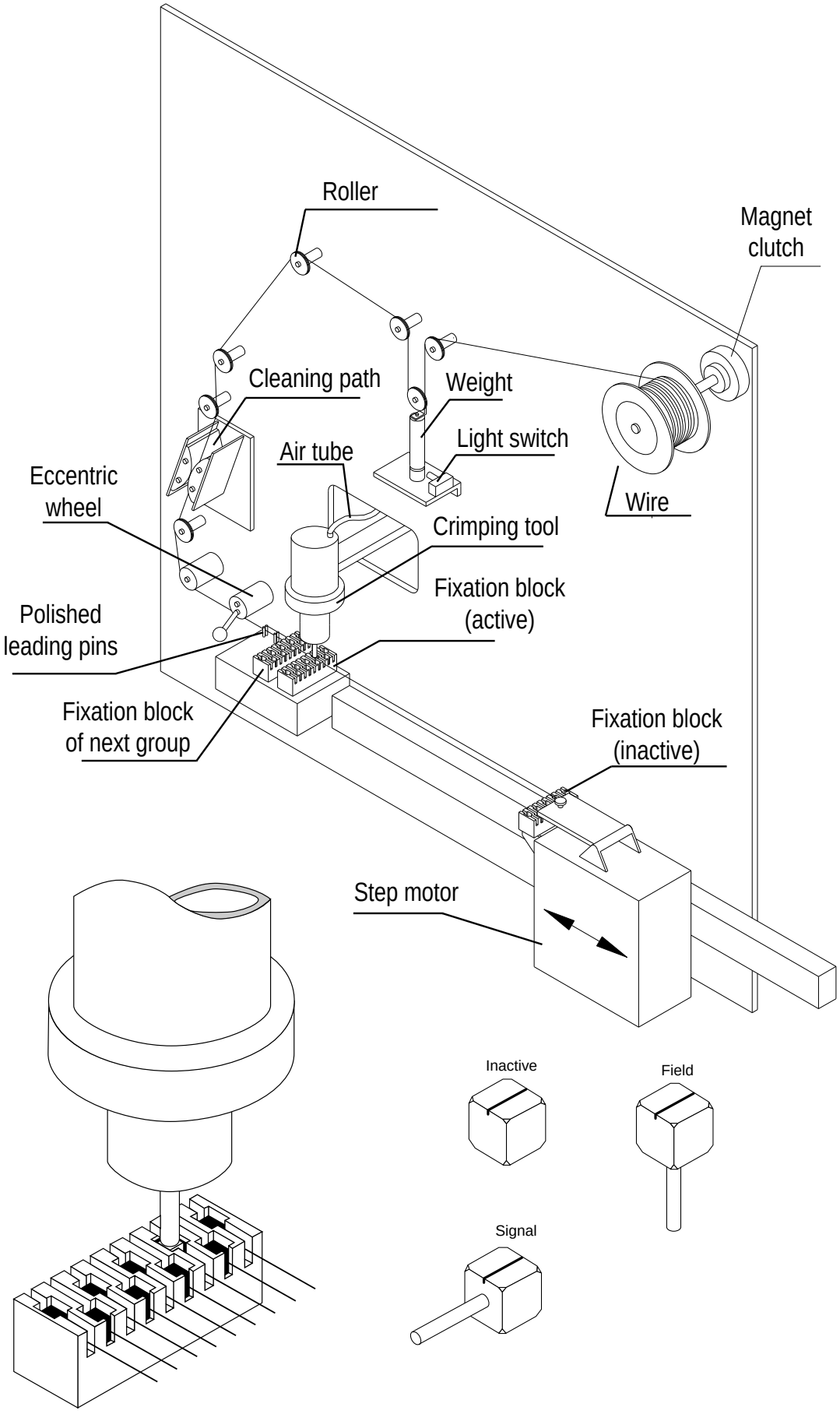
Roller
Magnet clutch
Cleaning path
Weight
Light switch
Air tube
Eccentric wheel
Wire
Crimping tool
Fixation block (active)
Polished leading pins
Fixation block of next group
Fixation block (inactive)
Step motor
Inactive
Field
Signal

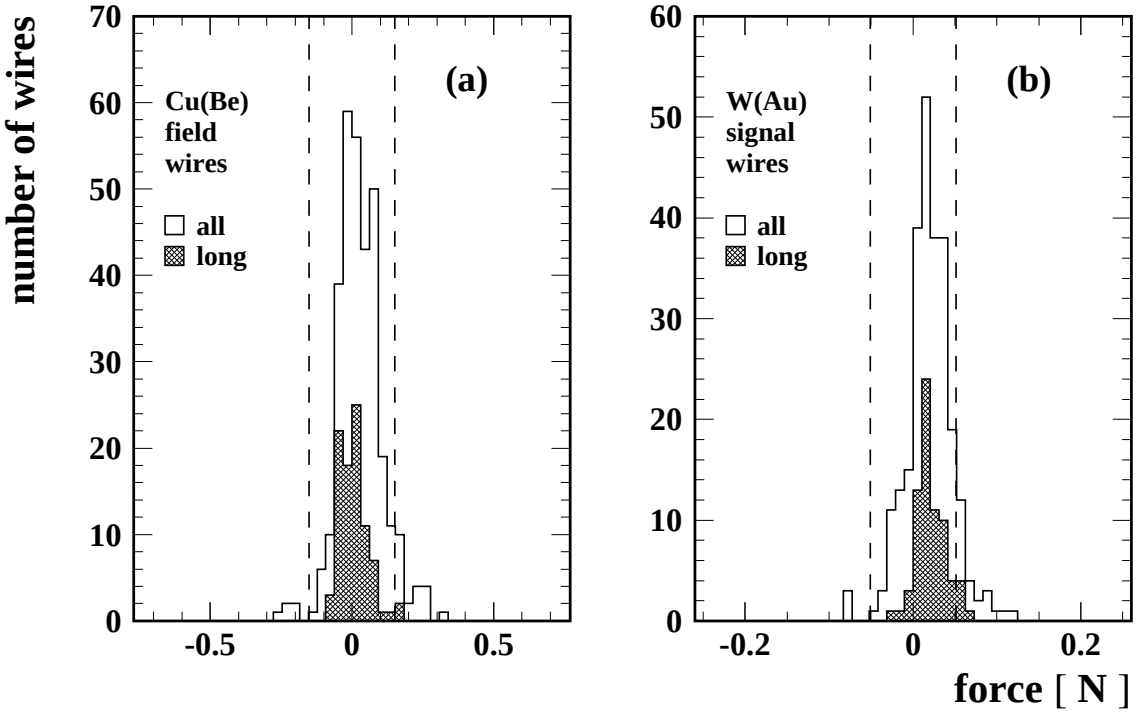
number of wires
70
60
50
40
30
20
10
0
-0.5
0
0.5
Cu(Be)
field
wires
all
long
(a)
60
50
40
30
20
10
0
-0.2
0
0.2
W(Au)
signal
wires
all
long
(b)
force [N]

±

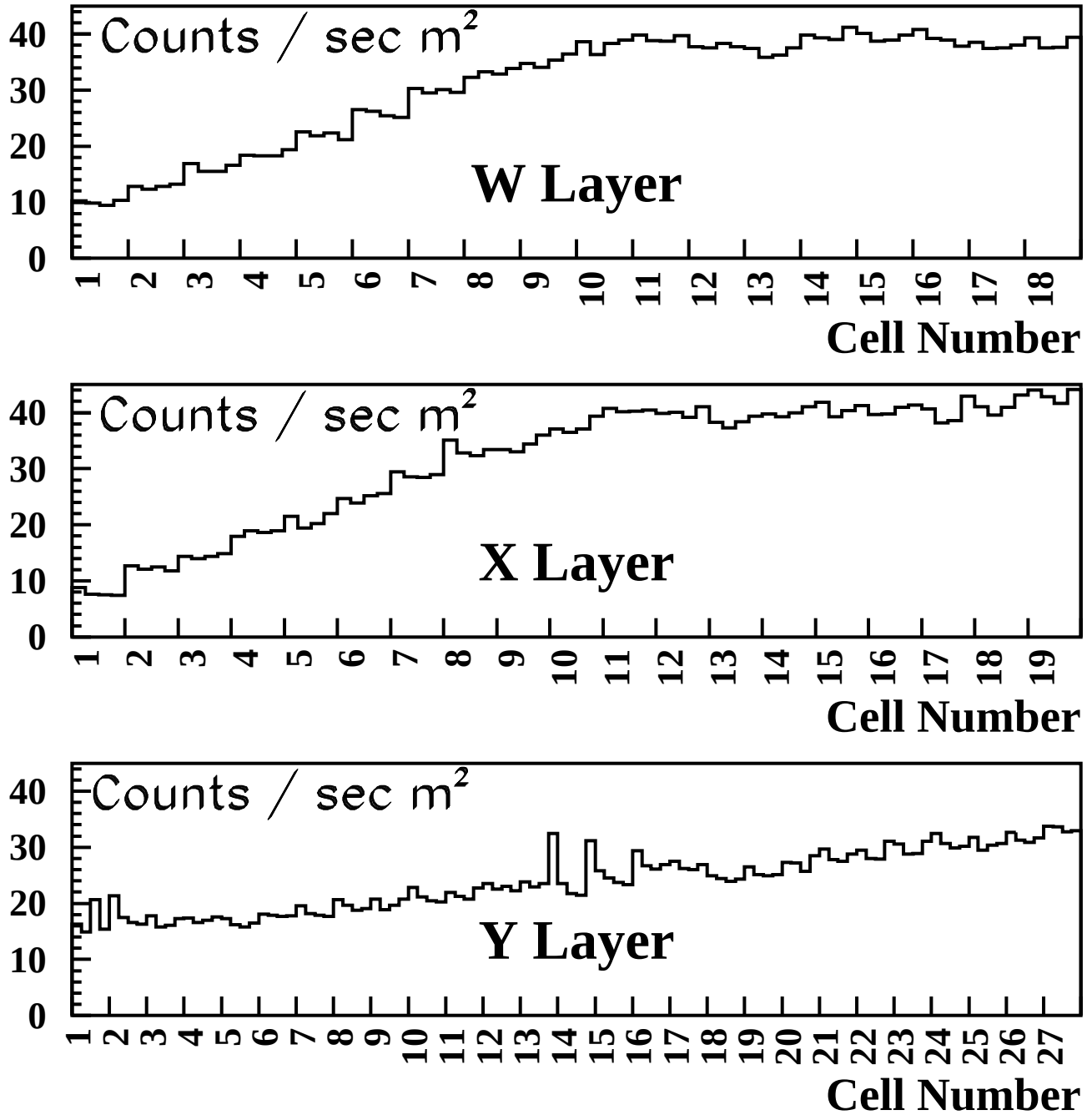
Counts / sec m²
W Layer
Cell Number
Counts / sec m²
X Layer
Cell Number
Counts / sec m²
Y Layer
Cell Number

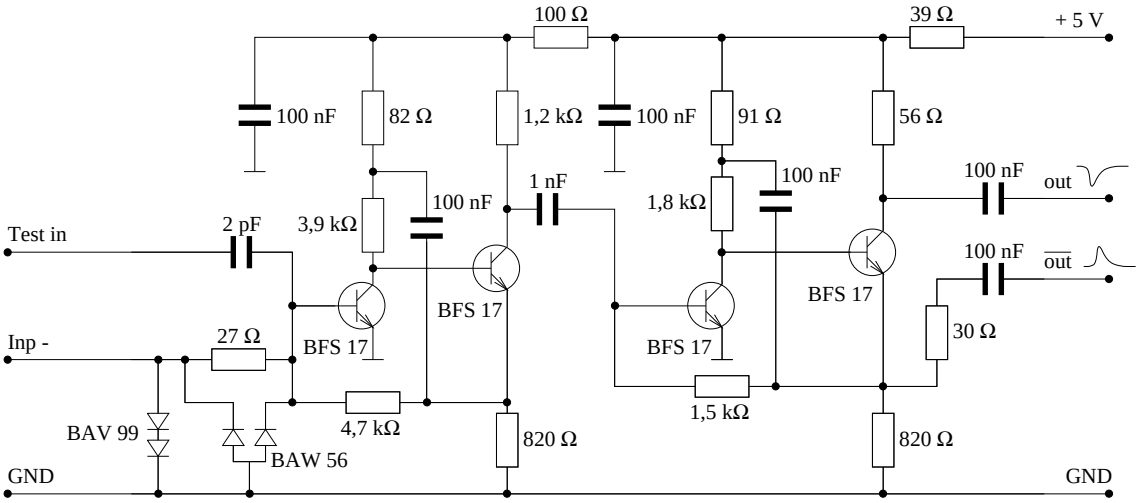
100 Ω
39 Ω
+ 5 V
100 nF
82 Ω
1,2 kΩ
100 nF
91 Ω
56 Ω
100 nF
out
1 nF
1,8 kΩ
100 nF
Test in
2 pF
3,9 kΩ
100 nF
100 nF
out
BFS 17
BFS 17
Inp -
27 Ω
BFS 17
30 Ω
BAV 99
4,7 kΩ
1,5 kΩ
820 Ω
820 Ω
BAW 56
GND
GND

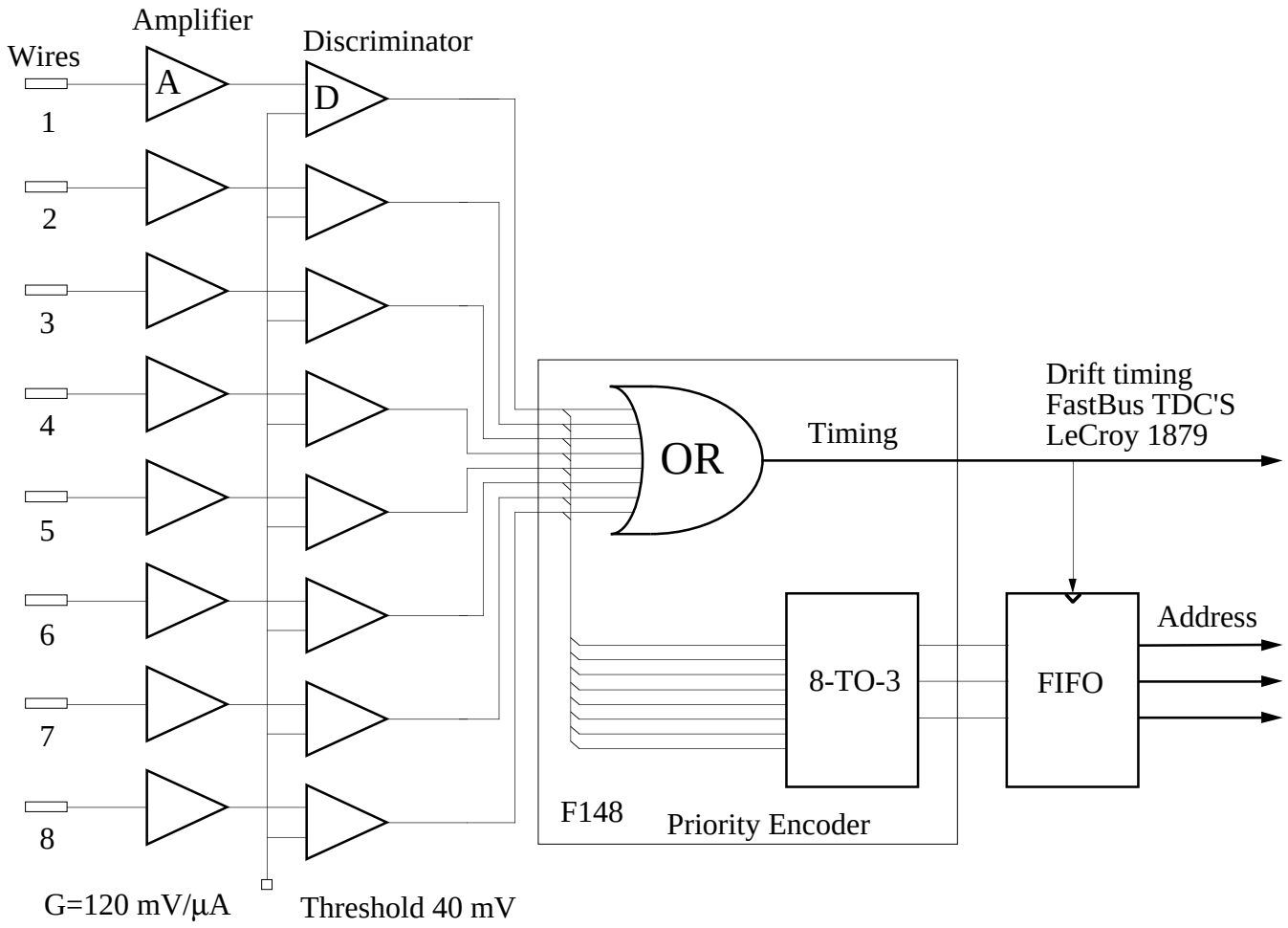
Amplifier
Discriminator
Wires
A
D
1
2
3
4
5
6
7
8
OR
Timing
Drift timing
FastBus TDC'S
LeCroy 1879
8-TO-3
FIFO
Address
F148
Priority Encoder
G=120 mV/μA
Threshold 40 mV

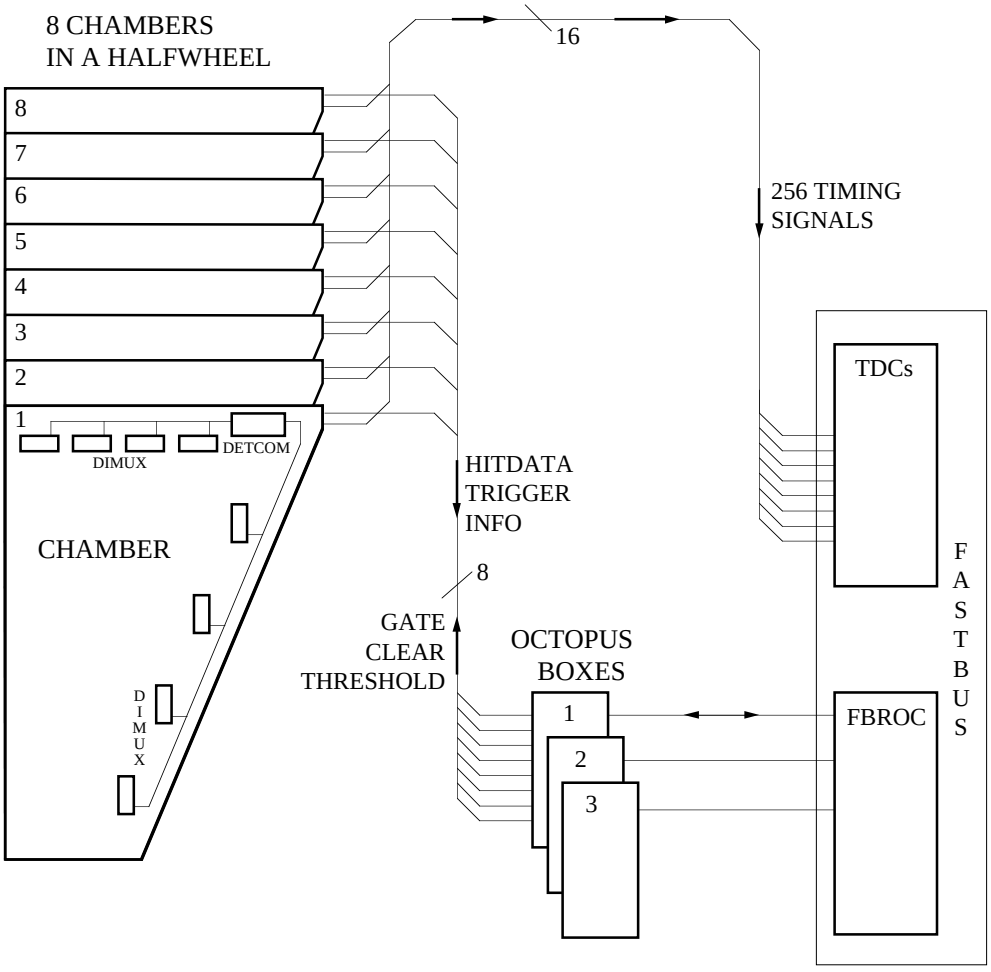
8 CHAMBERS
IN A HALFWHEEL
8
7
6
5
4
3
2
1
DIMUX
DETCOM
CHAMBER
DIMUX
16
256 TIMING
SIGNALS
HITDATA
TRIGGER
INFO
8
GATE
CLEAR
THRESHOLD
OCTOPUS
BOXES
1
2
3
TDCs
FBROC
FASTBUS

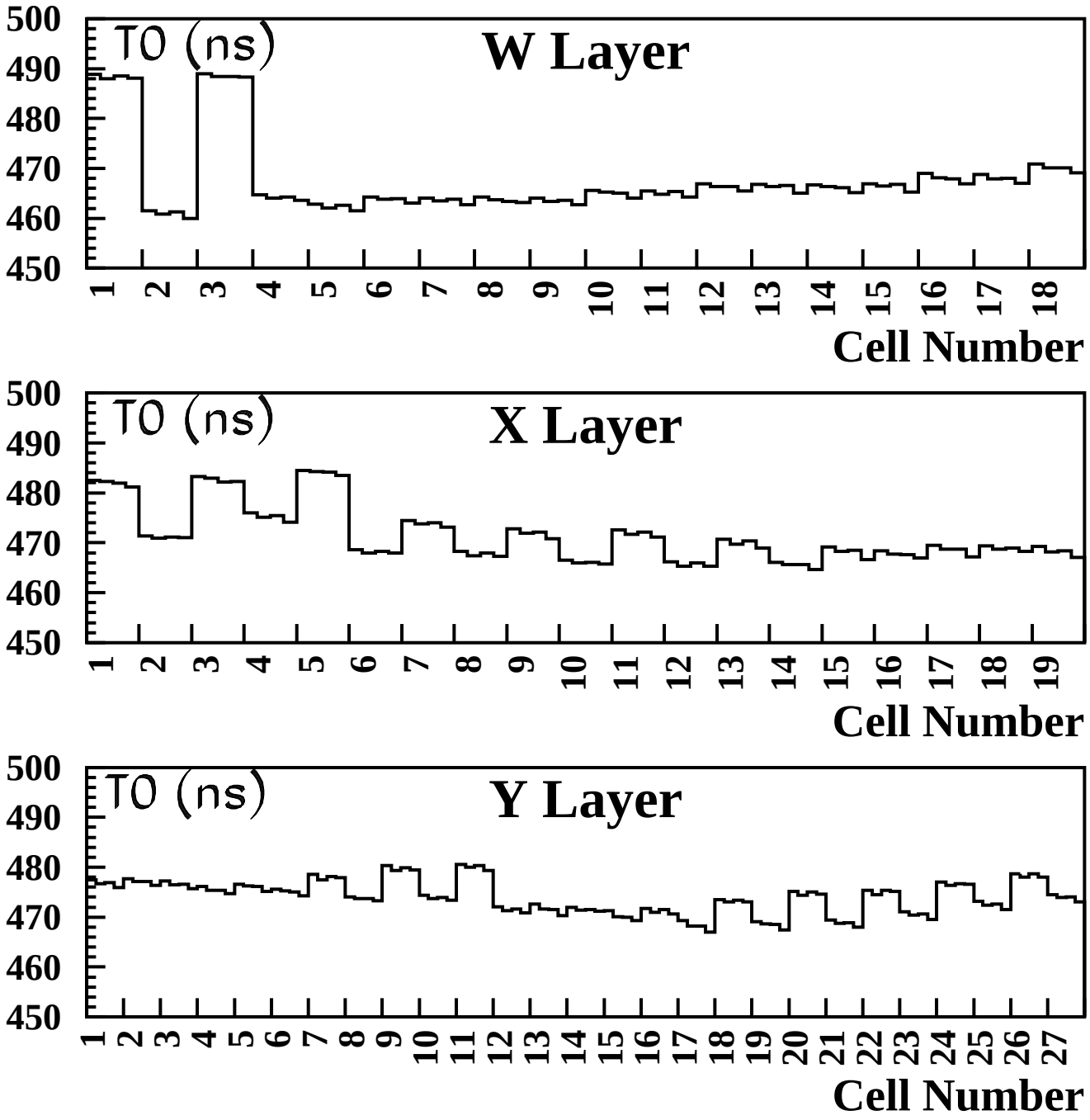
T0 (ns)
W Layer
500
490
480
470
460
450
1 2 3 4 5 6 7 8 9 10 11 12 13 14 15 16 17 18
Cell Number
T0 (ns)
X Layer
500
490
480
470
460
450
1 2 3 4 5 6 7 8 9 10 11 12 13 14 15 16 17 18 19
Cell Number
T0 (ns)
Y Layer
500
490
480
470
460
450
1 2 3 4 5 6 7 8 9 10 11 12 13 14 15 16 17 18 19 20 21 22 23 24 25 26 27
Cell Number

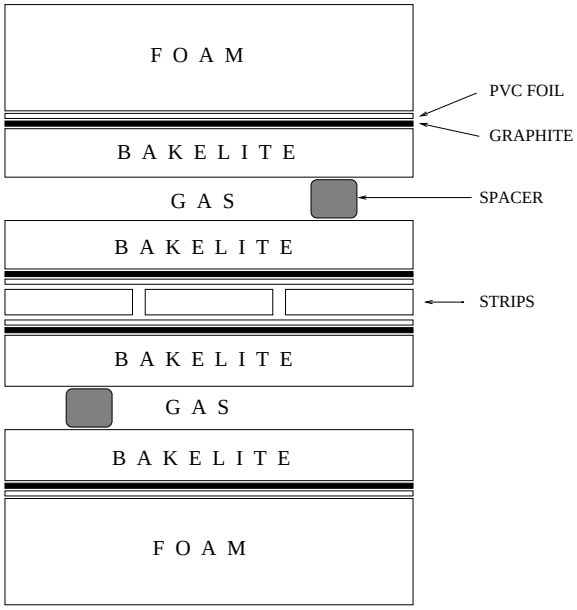
F O A M
PVC FOIL
GRAPHITE
B A K E L I T E
G A S
SPACER
B A K E L I T E
STRIPS
B A K E L I T E
G A S
B A K E L I T E
F O A M

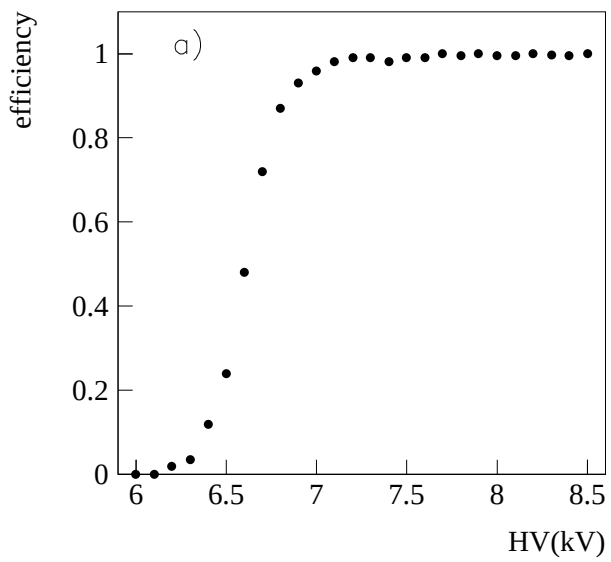
efficiency
a)
1
0.8
0.6
0.4
0.2
0
6
6.5
7
7.5
8
8.5
HV(kV)

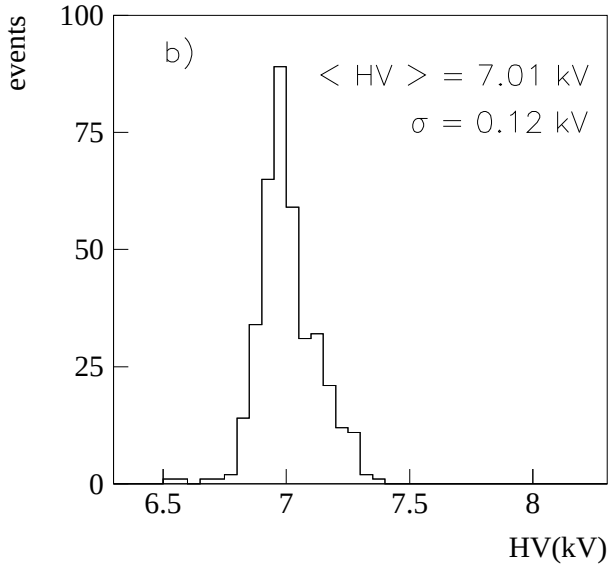
events
b)
< HV > = 7.01 kV
σ = 0.12 kV
100
75
50
25
0
6.5
7
7.5
8
HV(kV)

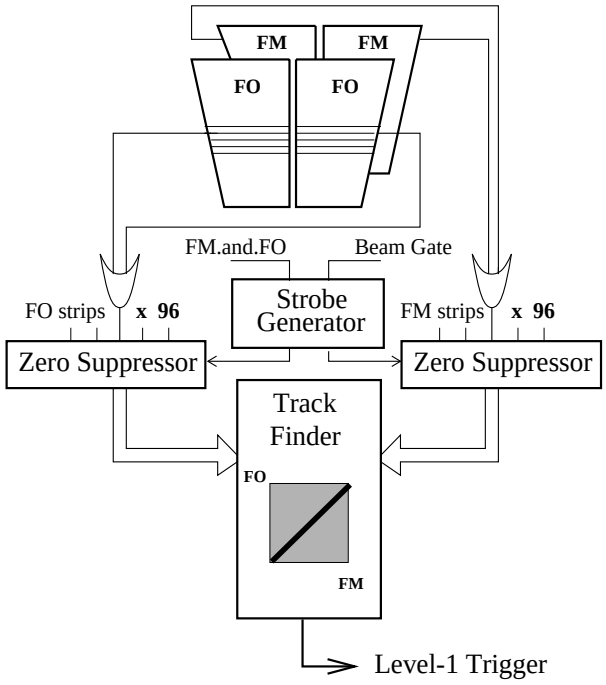
FM
FM
FO
FO
FM.and.FO
Beam Gate
FO strips
x 96
Strobe Generator
FM strips
x 96
Zero Suppressor
Zero Suppressor
Track Finder
FO
FM
Level-1 Trigger

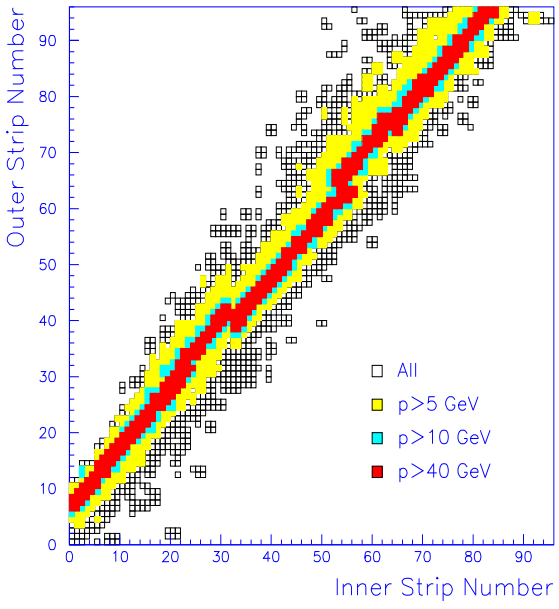
Outer Strip Number
Inner Strip Number
All
p>5 GeV
p>10 GeV
p>40 GeV
0
10
20
30
40
50
60
70
80
90

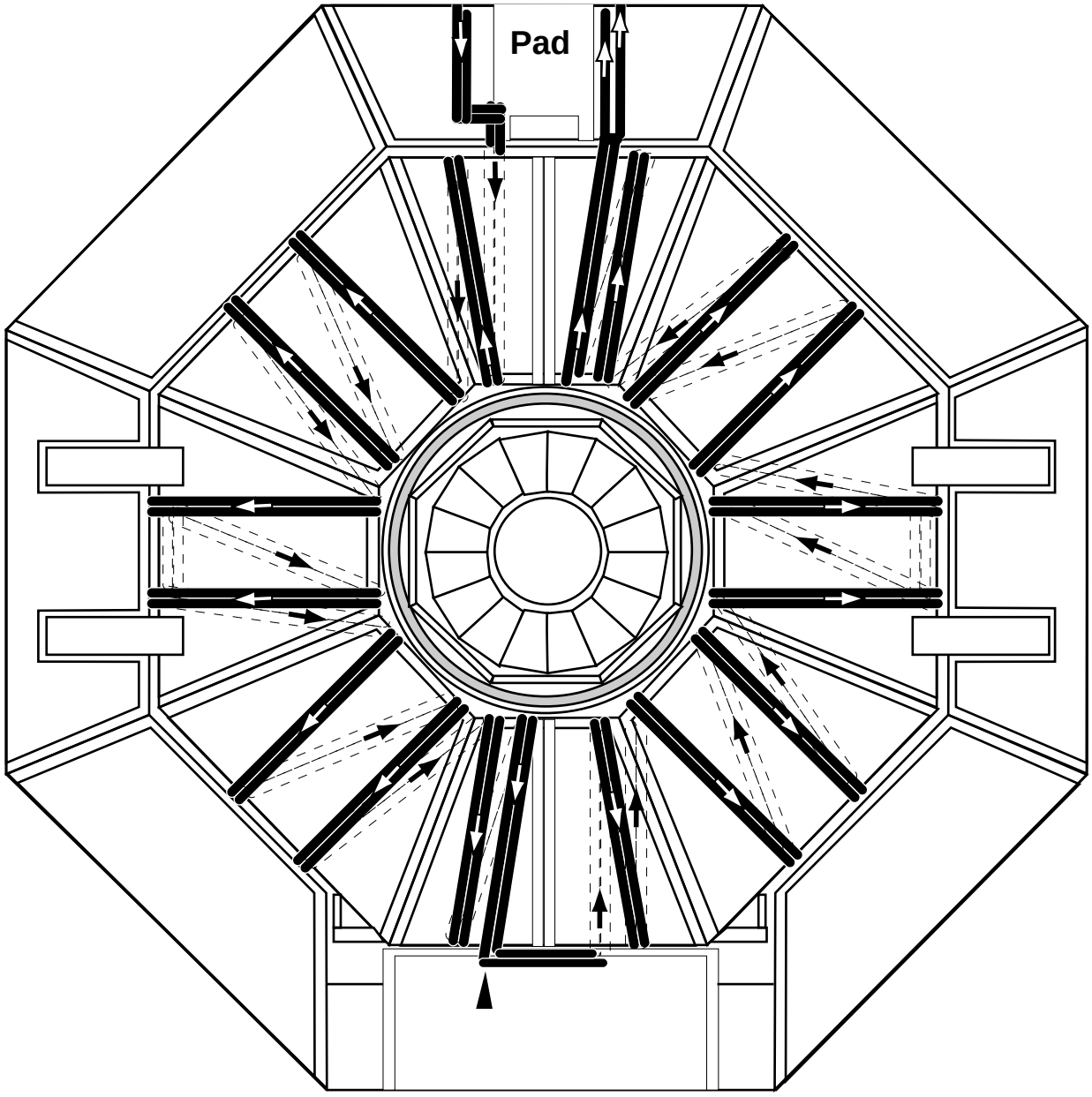
Pad

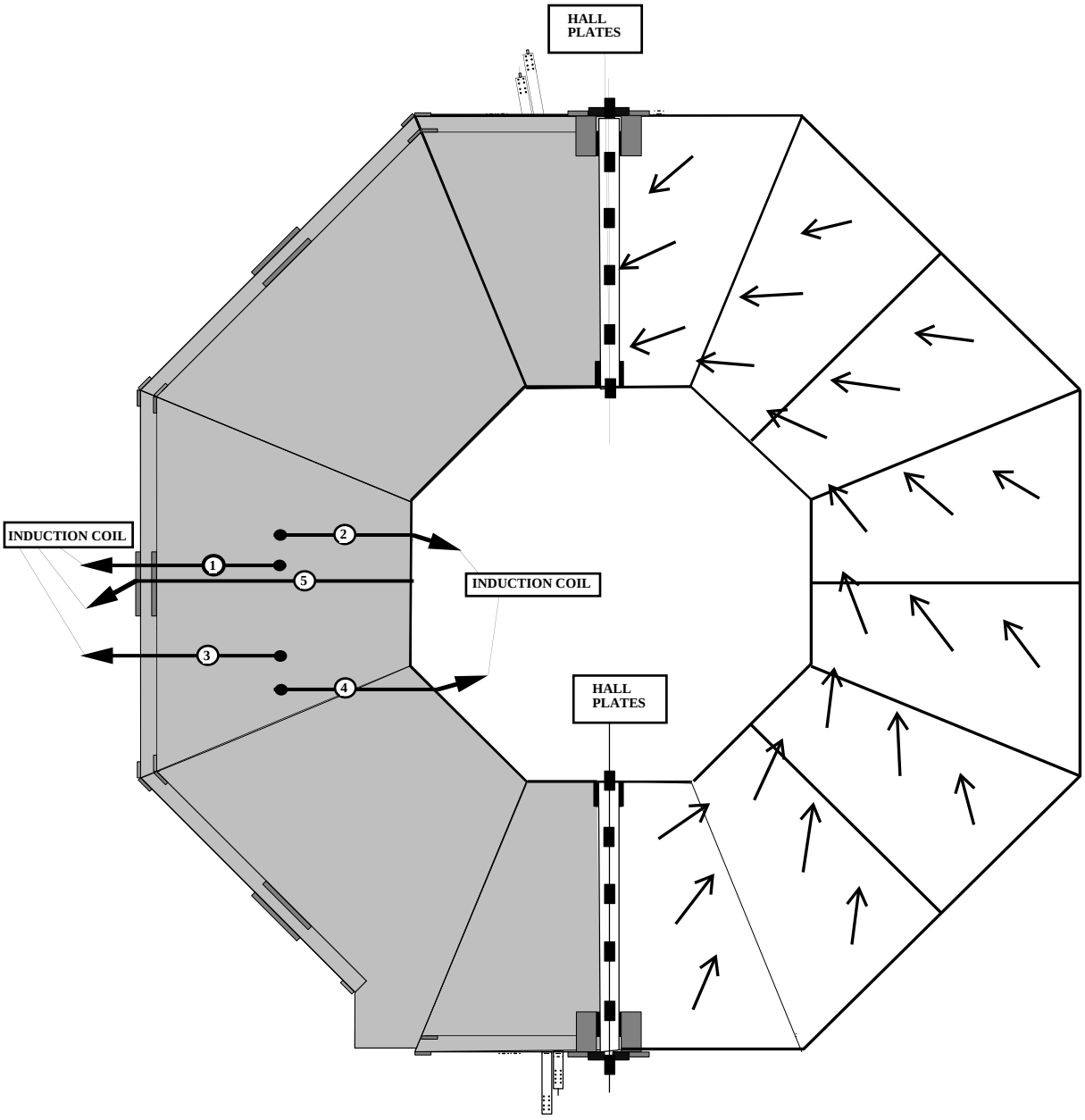
HALL PLATES
INDUCTION COIL
2
1
5
INDUCTION COIL
3
4
HALL PLATES

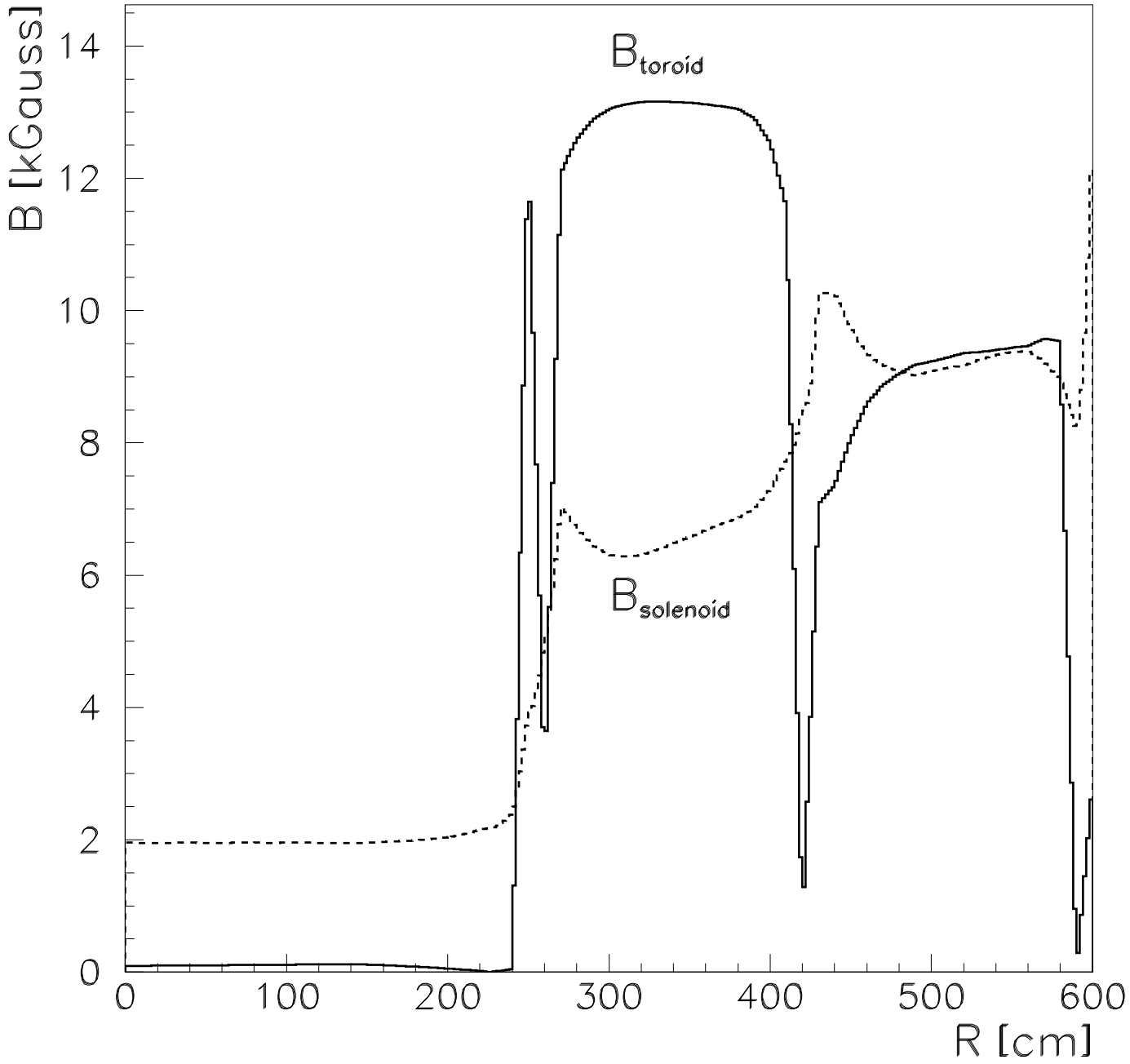
B [kGauss]
14
12
10
8
6
4
2
0
0
100
200
300
400
500
600
R [cm]
B toroid
B solenoid

°

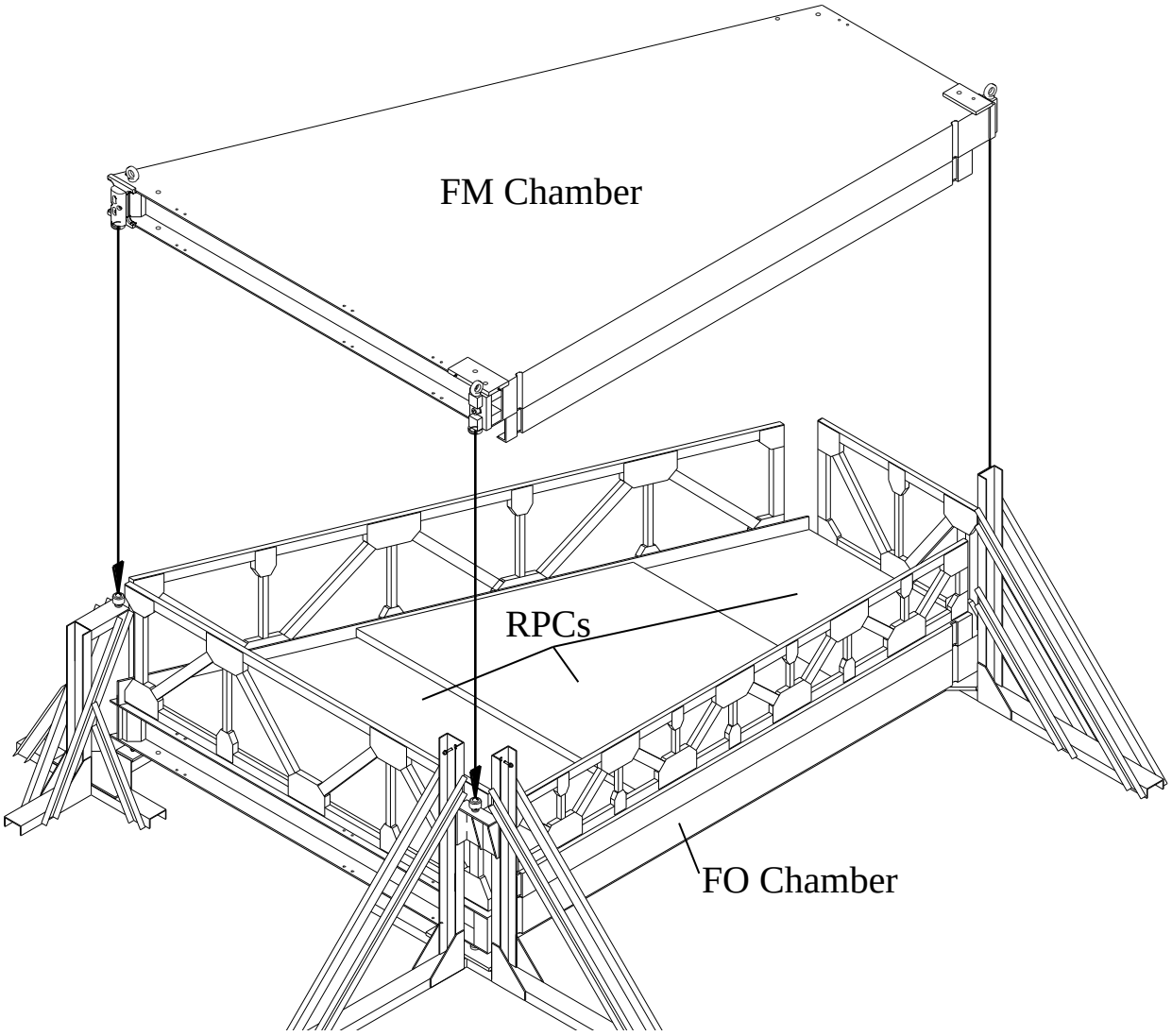
FM Chamber
RPCs
FO Chamber

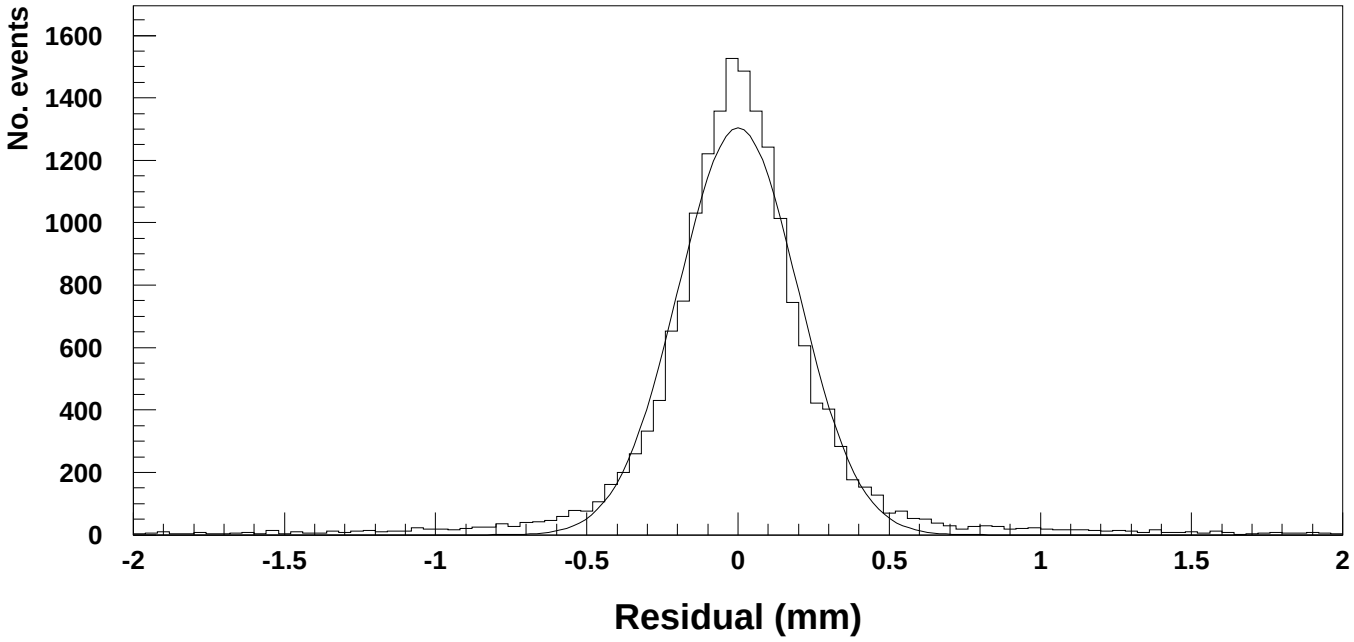

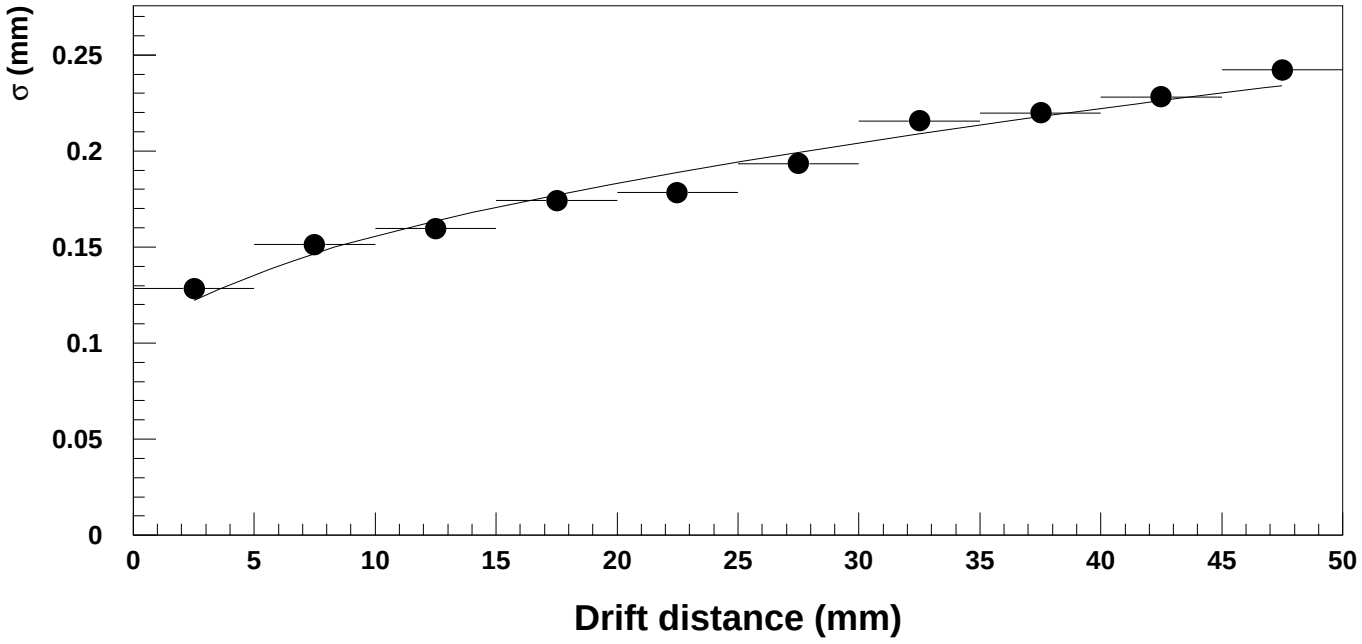

$$\sigma \times \sqrt{\frac{\mu}{\mu}} \qquad \sigma$$

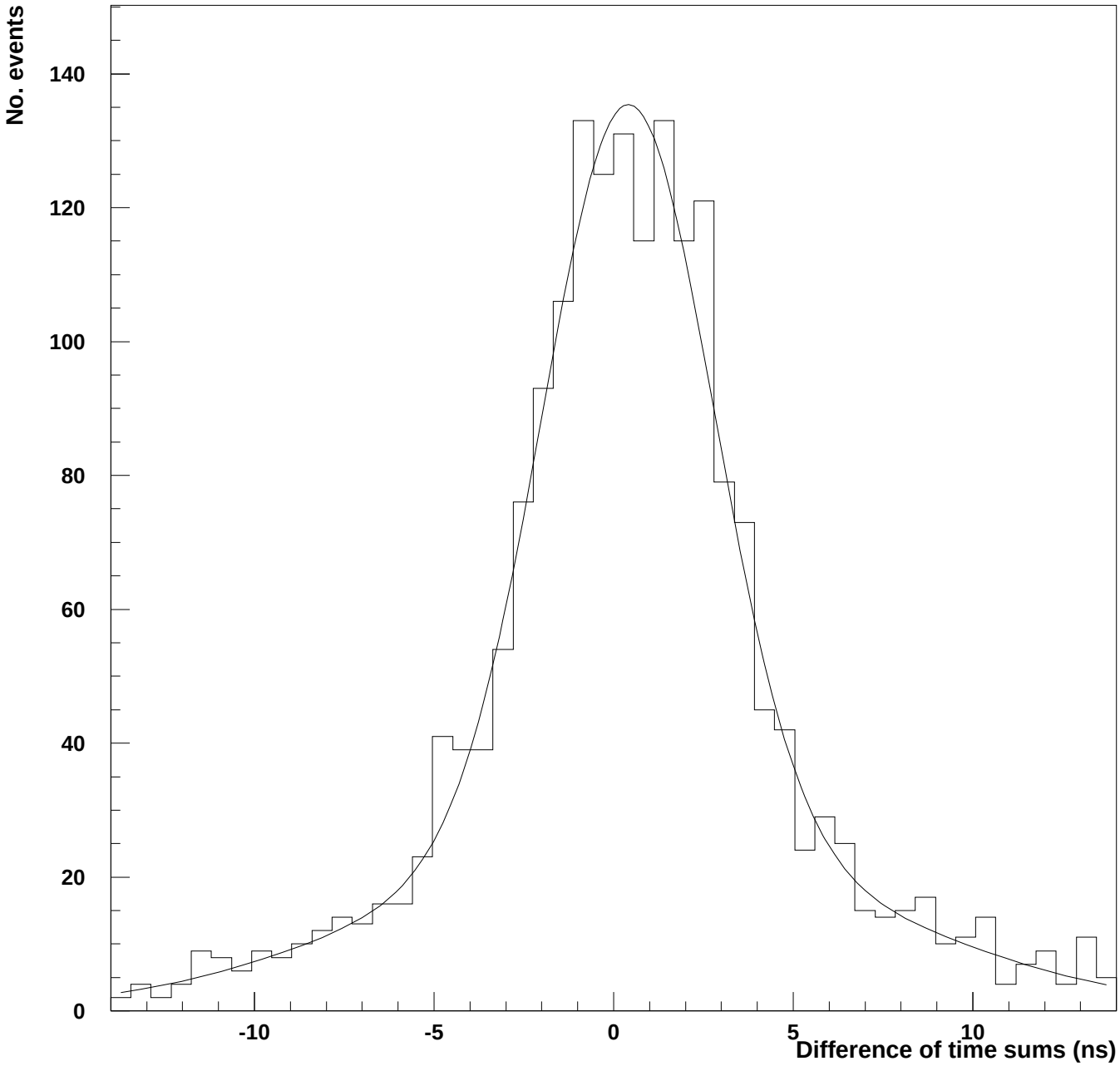
No. events
140
120
100
80
60
40
20
0
-10
-5
0
5
10
Difference of time sums (ns)

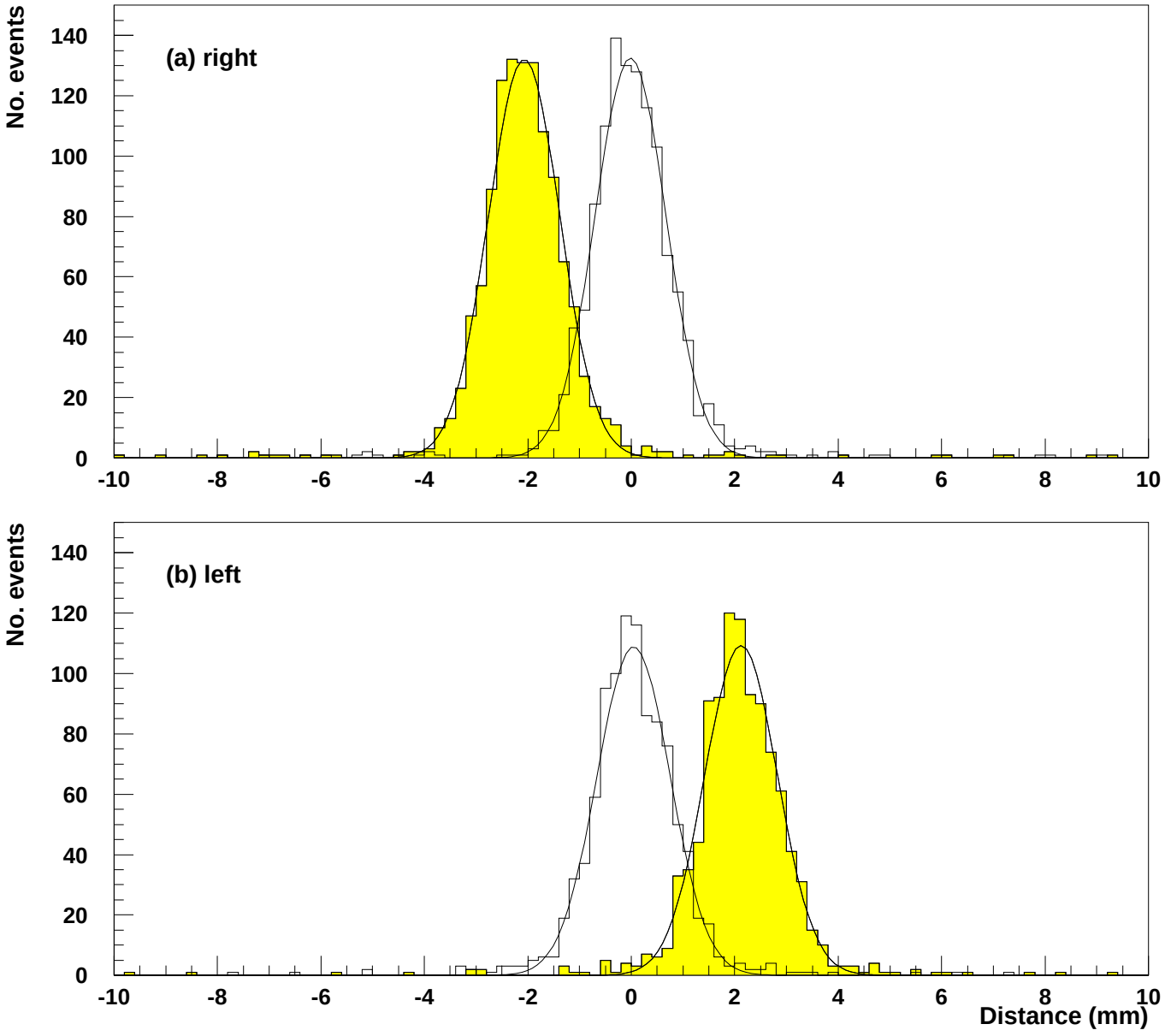
No. events
(a) right
140
120
100
80
60
40
20
0
-10
-8
-6
-4
-2
0
2
4
6
8
10
No. events
(b) left
140
120
100
80
60
40
20
0
-10
-8
-6
-4
-2
0
2
4
6
8
10
Distance (mm)

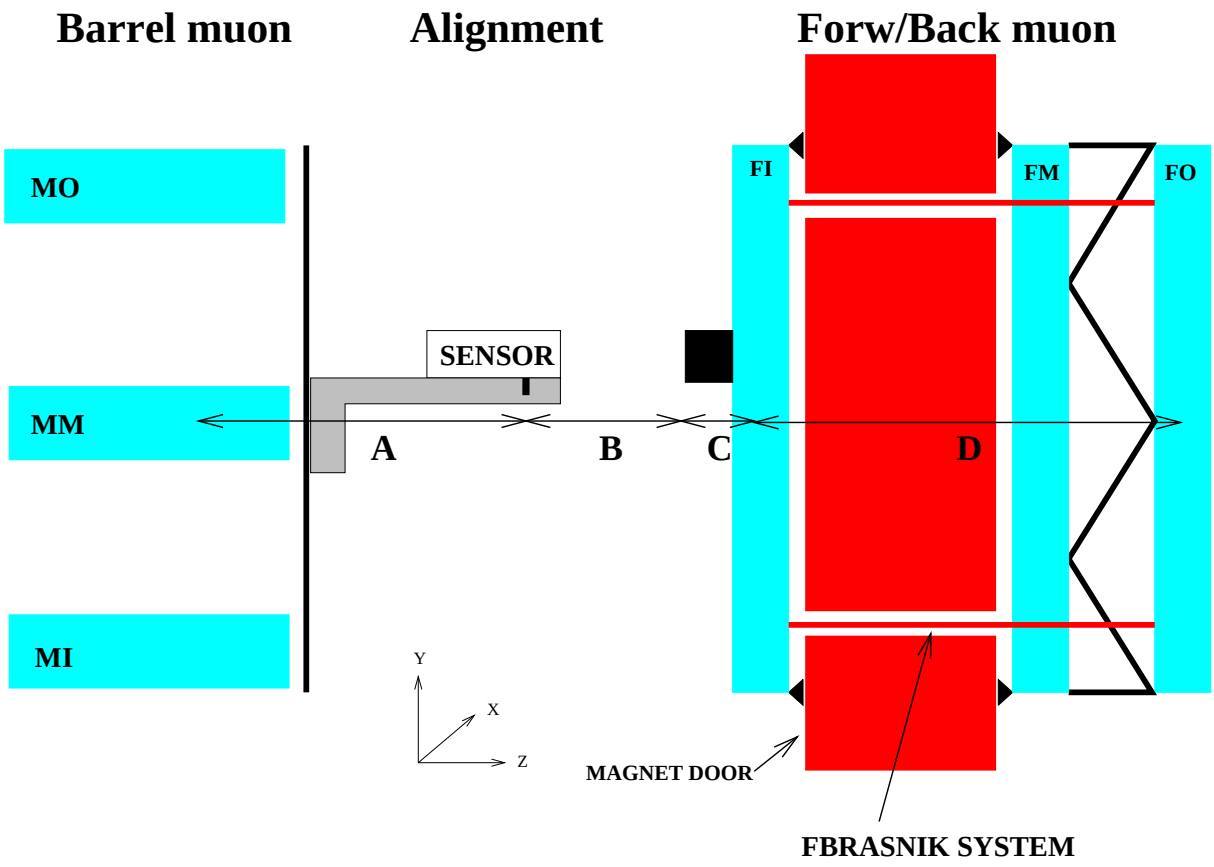
Barrel muon
Alignment
Forw/Back muon
MO
MM
MI
SENSOR
A
B
C
D
FI
FM
FO
Y
X
Z
MAGNET DOOR
FBRASNIK SYSTEM

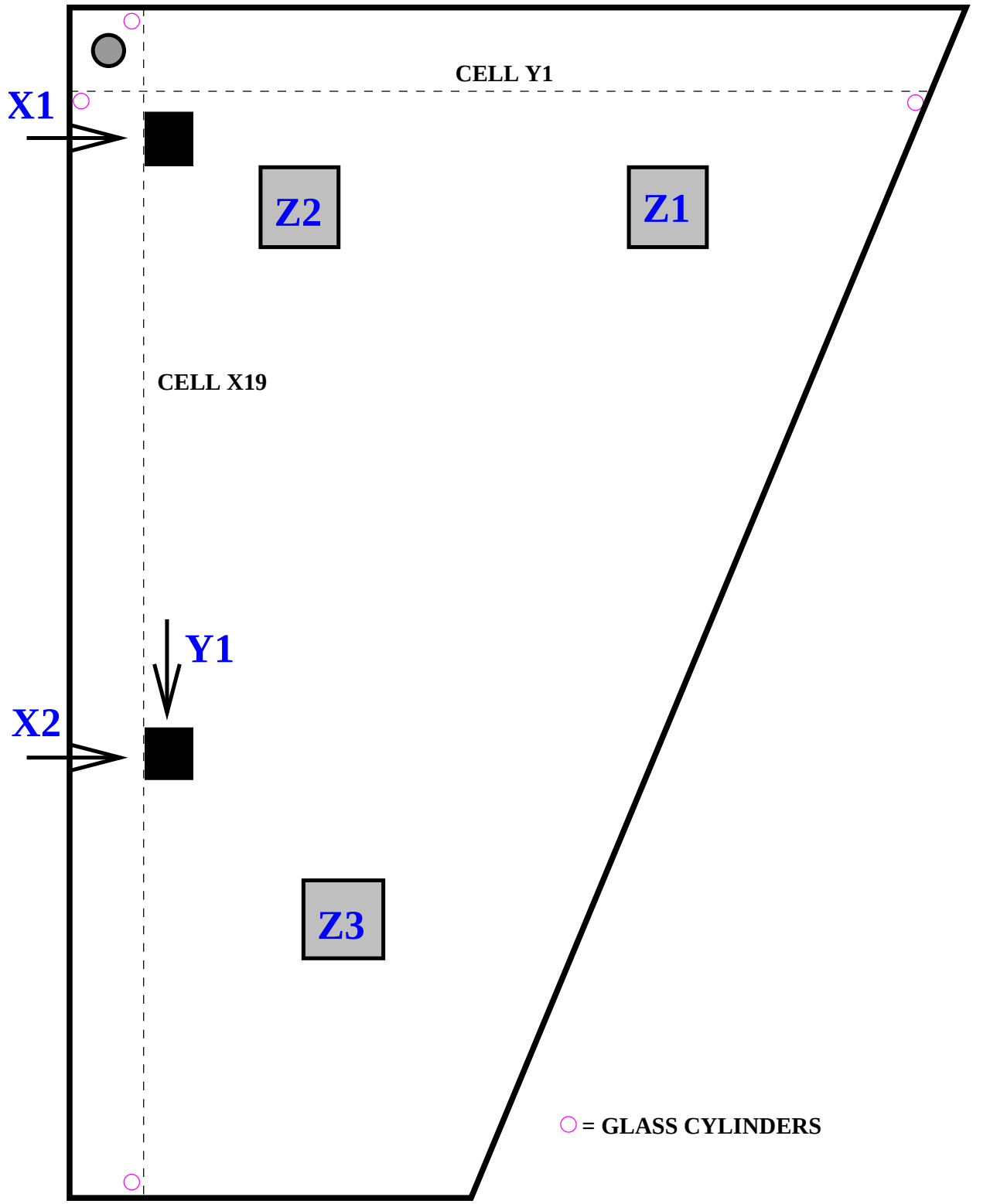

x y

z

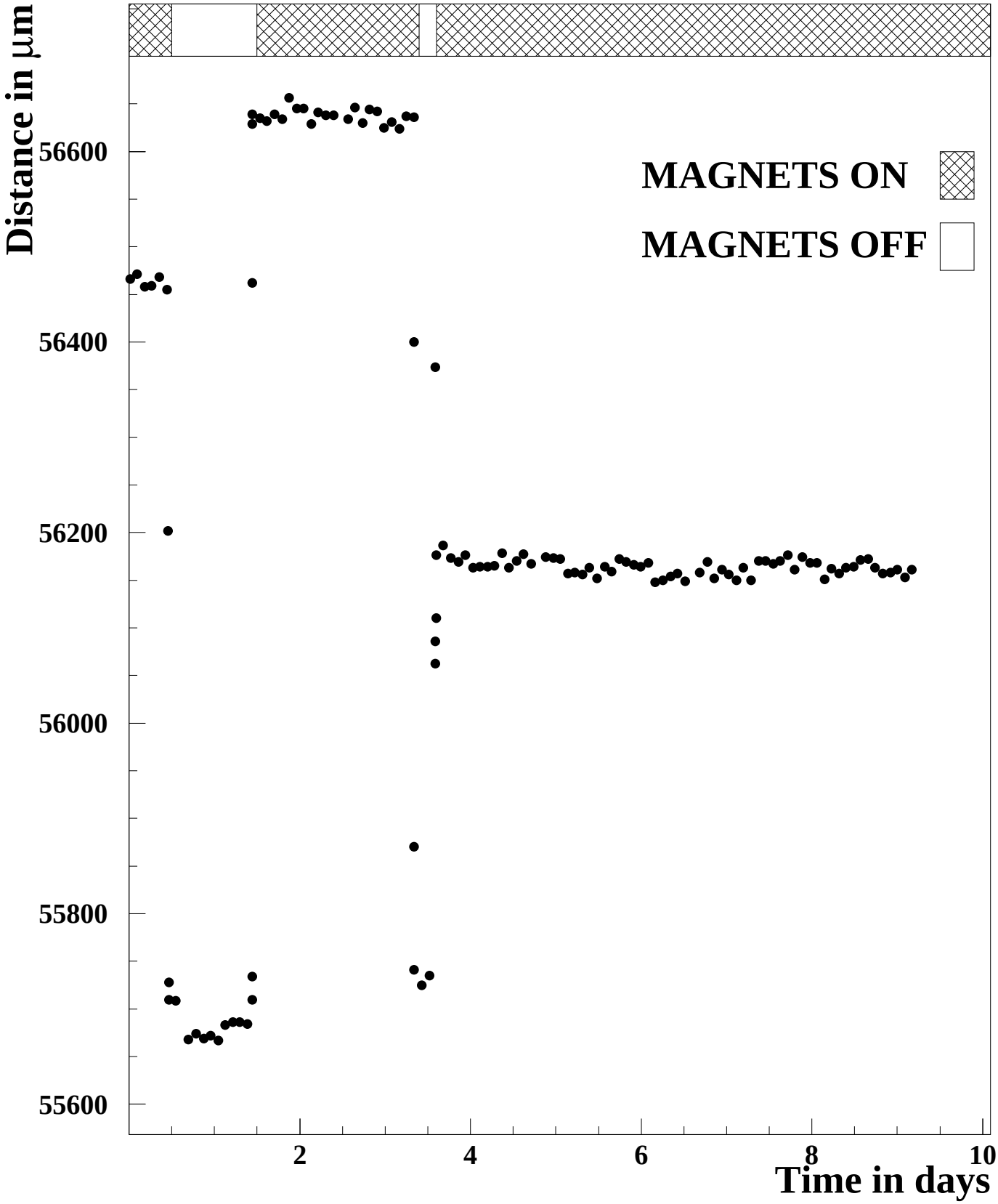
Distance in μm
56600
56400
56200
56000
55800
55600
MAGNETS ON
MAGNETS OFF
2
4
6
8
10
Time in days

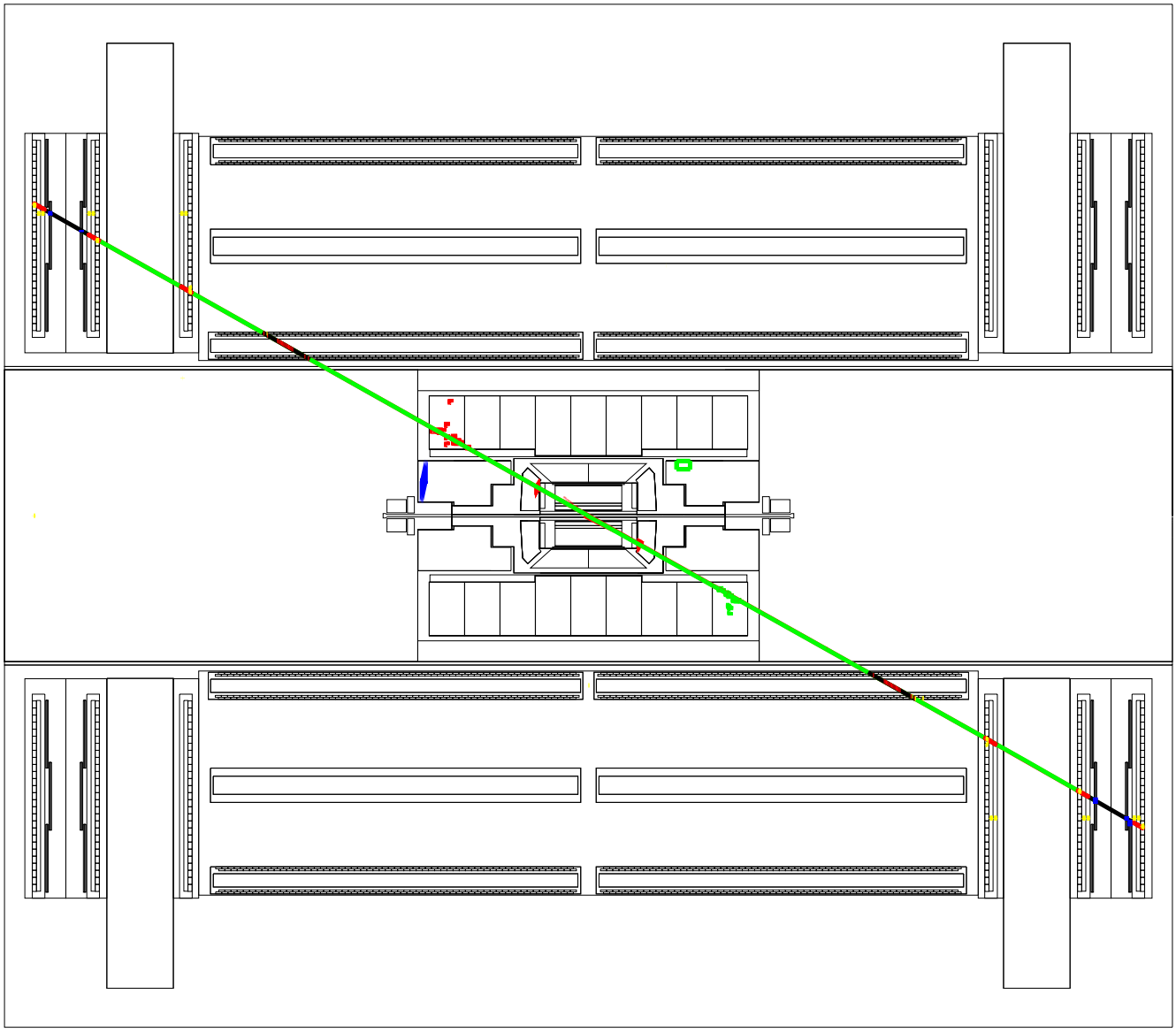

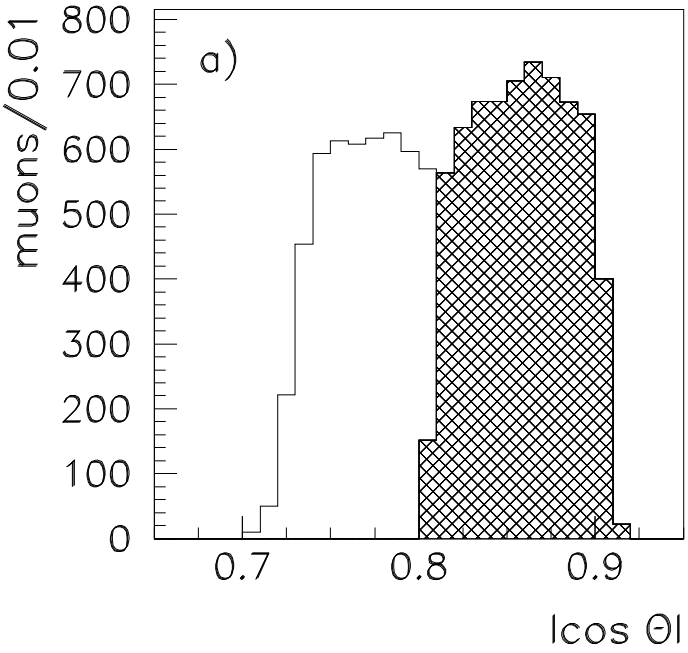
a)
muons/0.01
800
700
600
500
400
300
200
100
0
0.7
0.8
0.9
|cos Θ|

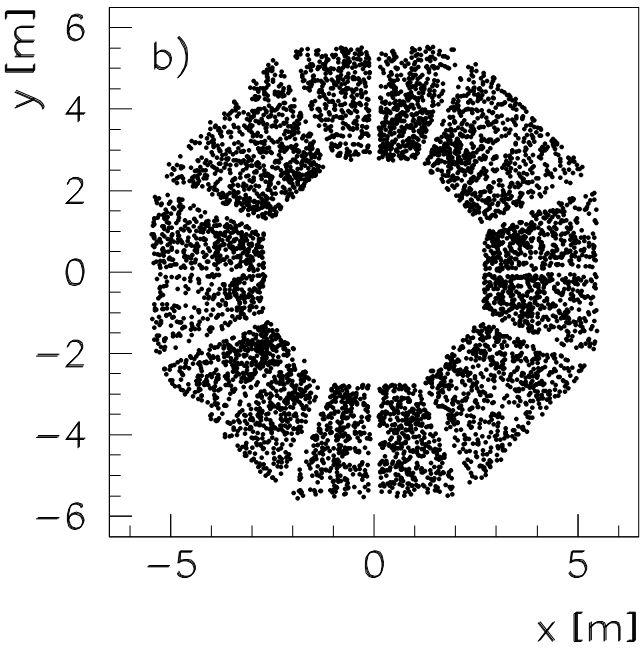
b)
y [m]
6
4
2
0
−2
−4
−6
−5
0
5
x [m]

$x - y$

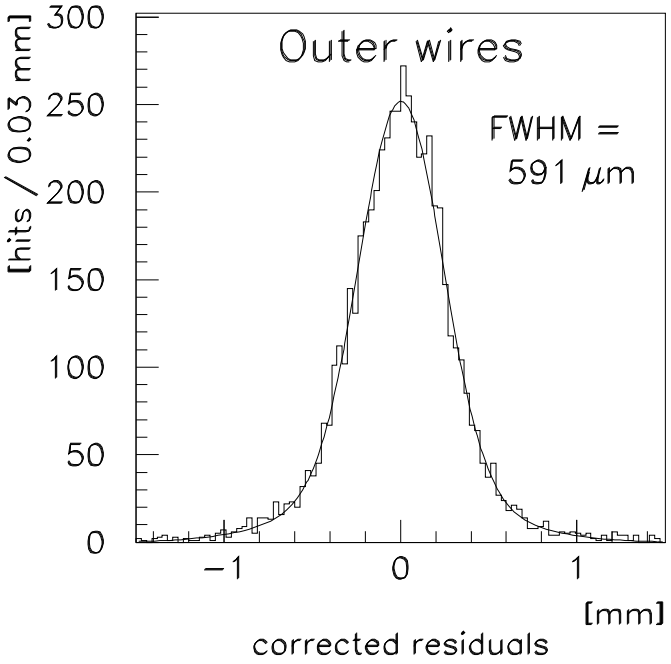
Outer wires
FWHM =
591 μm
[hits / 0.03 mm]
300
250
200
150
100
50
0
−1
0
1
[mm]
corrected residuals

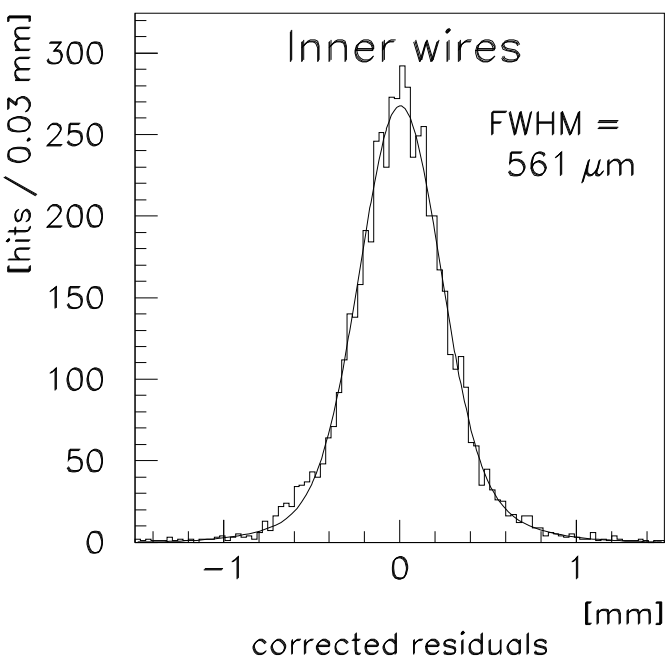
Inner wires
FWHM =
561 μm
[hits / 0.03 mm]
300
250
200
150
100
50
0
−1
0
1
[mm]
corrected residuals

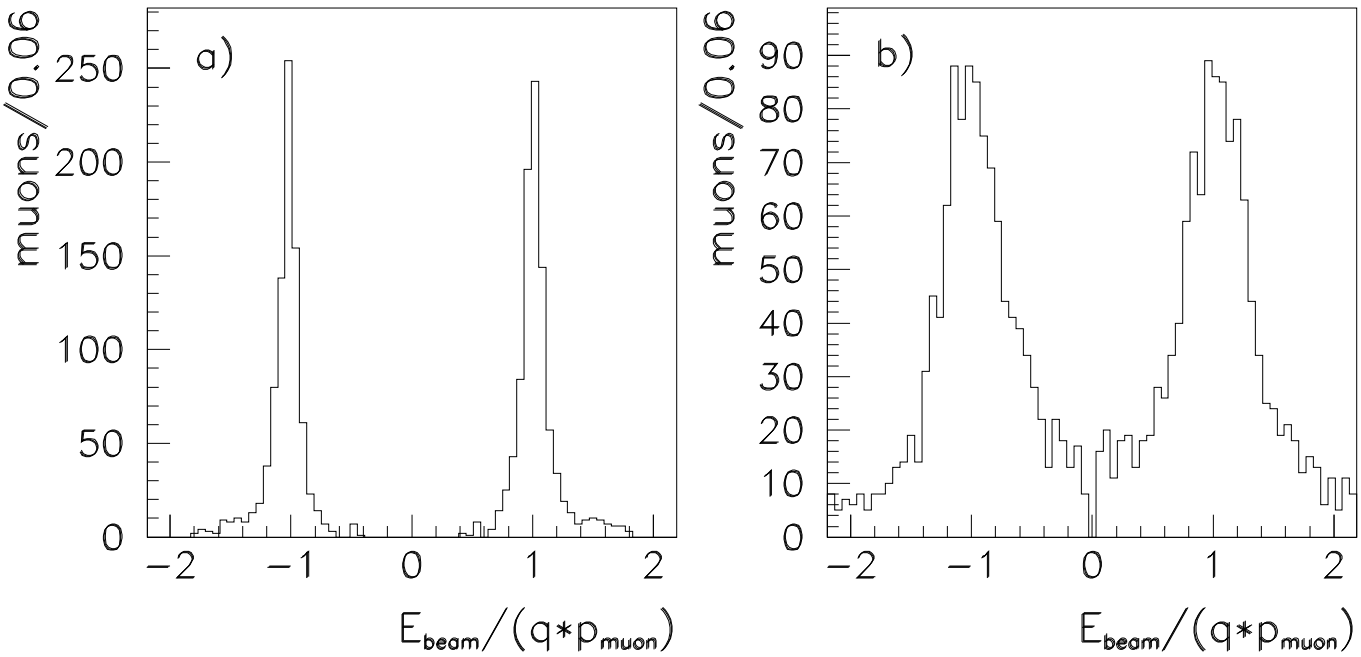

$e^+e^- \to \mu^+\mu^-\ \gamma$

$E_{beam}/\ q \cdot p_{muon}$ E_{beam} q

p_{muon}

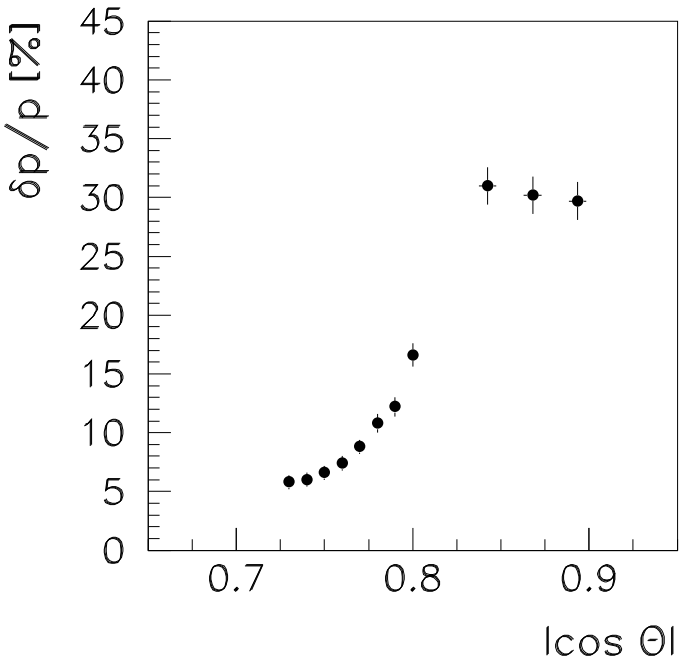
δp/p [%]
45
40
35
30
25
20
15
10
5
0
0.7
0.8
0.9
|cos Θ|

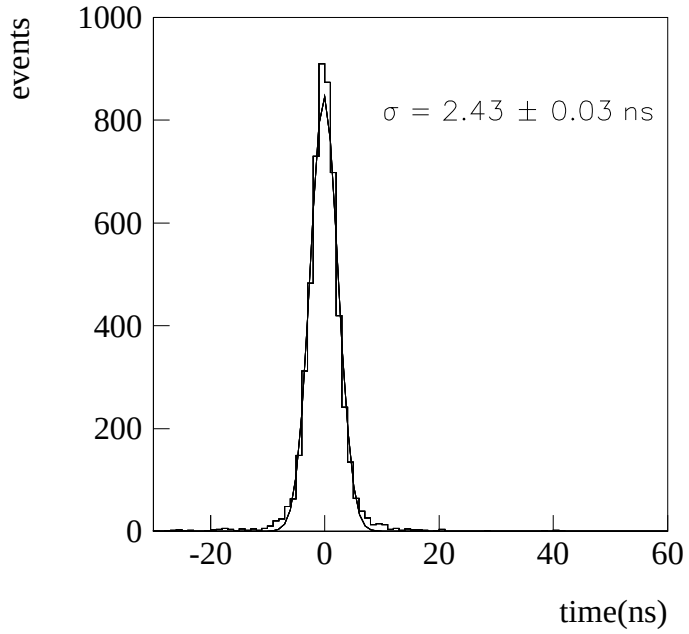
events
1000
800
600
400
200
0
σ = 2.43 ± 0.03 ns
-20
0
20
40
60
time(ns)

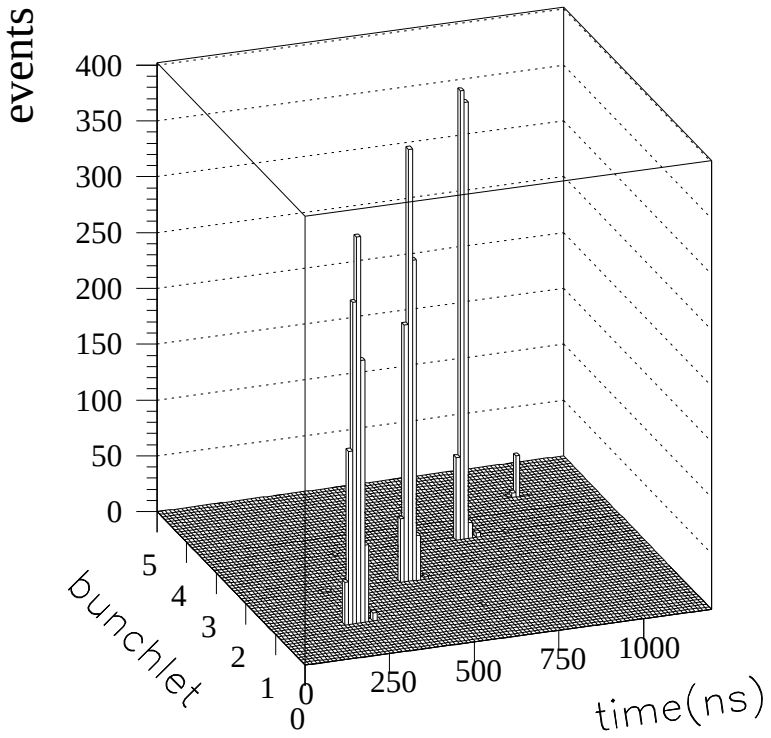
events
400
350
300
250
200
150
100
50
0
5
4
3
2
1
0
bunchlet
0
250
500
750
1000
time(ns)